VLÁKNA a TEXTIL

FIBRES AND TEXTILES

1

Volume 25.
March
2018

STU FCHPT

TECHNICAL UNIVERSITY OF LIBEREC
Faculty of Textile Engineering

Trenčianska univerzita Alexandra Dubčeka v Trenčíne
Fakulta priemyselných technológií v Púchove

VÚCHV

VÚTCH
CHEMITEX

Spoločnosť pre myselnej chémie
SVCH

CHEMOSVIT FIBROCHEM

Indexed in:
SCOPUS
Chemical Abstracts
World Textiles

ISSN 1335-0617
print version

ISSN 2585-8890
online version

Fibres and Textiles
Vlákna a textil

Published by

- Slovak University of Technology in Bratislava, Faculty of Chemical and Food Technology
- Technical University of Liberec, Faculty of Textile Engineering
- Alexander Dubček University of Trenčín, Faculty of Industrial Technologies
- Slovak Society of Industrial Chemistry, Bratislava
- Research Institute of Man-Made Fibres, JSC, Svit
- VÚTCH – CHEMITEX, Ltd., Žilina
- Chemosvit Fibrochem, JSC, Svit

Vydáva

- Slovenská technická univerzita v Bratislave, Fakulta chemickej a potravinárskej technológie
- Technická univerzita v Liberci, Fakulta textilní
- Trenčianska univerzita Alexandra Dubčeka v Trenčíne, Fakulta priemyselných technológií
- Slovenská spoločnosť priemyselnej chémie, Bratislava
- Výskumný ústav chemických vlákien, a.s. Svit
- VÚTCH – CHEMITEX, spol. s r.o., Žilina
- Chemosvit Fibrochem, a.s., Svit

Editorial office and distribution of the journal
(Redakcia a distribúcia časopisu)

Ústav prírodných a syntetických polymérov
Fakulta chemickej a potravinárskej technológie
Slovenská technická univerzita v Bratislave
Radlinského 9, 812 37 Bratislava, SK
Tel: 00 421 2 59 325 575
e-mail: marcela.hricova@stuba.sk

Order and advertisement of the journal
(Objednávka a inzercia časopisu)

Slovenská spoločnosť priemyselnej chémie,
člen Zväzu vedecko-technických spoločností
Radlinského 9, 812 37 Bratislava, SK
Tel: 00 421 2 59 325 575
e-mail: marcela.hricova@stuba.sk

Order of the journal from abroad – excepting Czech Republic
Objednávka časopisu zo zahraničia – okrem Českej Republiky

SLOVART G.T.G, s.r.o. EXPORT-IMPORT
Krupinská 4, P.O.Box 152, 852 99 Bratislava, SK
Tel: 00421 2 839 471-3, Fax: 00421 2 839 485
e-mail: info@slovart-gtg.sk

Typeset and printing *(Sadzba a tlač)*

FOART, s.r.o., Bratislava

Journal is published 4x per year
Subscription 60 EUR

Časopis vychádza 4x ročne
Ročné predplatné 60 EUR

Evidenčné číslo MKCR SR Bratislava EV 4006/10

Fibres and Textiles (1) 2018
Vlákna a textil (1) 2018

March 2018

Content

COSTUME DESIGNIN FOR HOSPITALITY ESTABLISHMENTS STAFF ON THE BASIS OF ANALYSIS THE SLAVIC SNAKES ORNAMENTATION

Mariia Artemenko[1], Olena Yakymchuk[1], Dmytro Yakymchuk[2], Nadiia Myrhorodska[1] and Iryna Zasornova[3]

[1]Kherson National Technical University, Berislav highway 24, Kherson, Ukraine
[2]Kherson State University, 40 rokiv Zhovtnya St. 27, Kherson, Ukraine
[3]Khmelnitsky National University, Institytska str. 11, Khmelnitskyi, Ukraine
marikomash@gmail.com; lesya_popovich@mail.ru; starcon84@gmail.com; myrhorodska@i.ua; izasornova@gmail.com

Abstract: *Conducted research of leather ornamentation of Slavic snakes through graphical analysis picture populations of snakes, living in the territory of modern Ukraine. Developed following recommendations for the principles of constructing the Slavic snakes compositions in designing a women's and men's suit. Developed design-suggestions for men's and women's costumes for waiters who work in hospitality establishments. Investigated that they are conceptually focused on identifying regional peculiarities in their activities.*

Keywords: *Slavic snakes, ornamentation, suit designing, hospitality establishments, costume in tourism.*

1 INTRODUCTION

Suit in general and clothes in particular is one of the key components of subject-spatial human world. It allows not only satisfy the utilitarian and practical needs, but also acts as a powerful means of communication and identification. By clothes can determine the gender, age, national and cultural affiliation, social status, occupation of his owner, etc. These suit features today are actively used in advertising technology, positioning one or another brand, product or service.

Hospitality facilities today are an integral part of tourism and recreation, which have recently been rapidly developing and becoming priorities in the economic and cultural development of the regions. The region itself with its unique natural-climatic and national-cultural peculiarities becomes a sort of commodity that needs to be identified in the hard conditions of global integration and globalization.

Such situation requires from the administration of hospitality facilities reorientate to conceptual design, which will reflect the specifics of the region, both in interiors and landscapes, and in the artistic images of its employees.

Obviously, using a suit to solve the issue of identifying the territory and promoting it as a tourist product is a matter of relevance. Therefore, it requires a profoundly comprehensive analysis of the peculiarities of the regions (climatic conditions, flora, fauna, cultural heritage, peculiarities of the mentality, etc.). Also is need further develop of recommendations for application obtained results in designing unique uniforms and designs of clothes for different purposes. They can be used as a means of achieving artificial tourist attractions. This is the clothes of service workers, and a spectacular suit for party show programs in recreational activities and clothing of mass destination for residents of a given region.

A powerful inspiration for the conceptual design of hospitality facilities and various tourist products is mythology, the ancient epic and folk traditions. They determine the uniqueness and originality of the cultural development of the region. Quite often, the primary source in formation of mythological notions of the universe in cultures of many nations is the animal world.

In this article, for the purpose of clothes designing is paid attention to investigation of ornamental structure of snake's skin living on the Ukraine territory. The motivating factor was that the image of the Snake in Trypillian, Scythian and Slavic culture occupied one of the leading places. Therefore, it can be used in the design of various tourist products that are suit conceptually created.

In addition, the snake motives and images are in today's trend and find its application in many areas of modern design – clothing, interior, architecture, graphic design, etc. However, the consumer of the twenty-first century demands from the manufacturer a more profound rethinking and a new vision.

In order to achieve this goal, it is necessary to look for new artistic solutions or to provide new qualities to already existing developments.

There are many scientific papers on the topic of the chosen field of study [1-11]. Work [1] is devoted to the development of a costume for tourist attractions in Thailand, and [2] – describes the issue of a traditional costume of a particular region of China. The authors of the article [3] consider modern avant-garde costume in the aspect of design from a variety of topical problems. At the same time, the main attention focused on the designer components of the investigation. Some works [4, 5] describe specific characters of fairy tales and reflect the peculiarities of their visual component.

The research [6] aims at studying the problems of images of Slavic myths with an emphasis on establishing specific features of their description. Works [7, 8] are devoted to modern technologies of snake skin simulation. They describe a deep coloristic analysis of snake skin, and consider the ornamental-texture components of the images of Slavic snakes.

Worth to note, that there is a significant number of works [9-11] devoted to the study of specific components of hospitality industry in the aspect of development of modern suits design-projection for their staff. However, they do not describe the ornamentation of Slavic snakes. This significantly impairs development of a modern costume for hospitality establishments considering the investigated aspect.

Therefore, there is necessity to develop recommendations for the design of modern suit for hospitality establishment's staff on the basis of analysis of Slavic snake's ornamentation.

2 EXPERIMENTAL

Investigation of leather ornamentation of Slavic snakes conducted through graphical analysis picture populations of snakes, living in the territory of modern Ukraine. Graphic analysis included identifying the basic structural elements and the principles of their organization with further systematization of the obtained results and the construction of typical schemes, which can relayed to the design of clothing models. All of these analytic operations were performed in a CorelDraw vector graphic editor environment.

The population of East Slavic snakes in general includes 11 species of snakes, which relate to 2 families – the vipers and grass snakes. The most complete variety of snakes inhabits the territory of modern Ukraine – all 11 species (Figure 1).

At the first stage of the study, in order to specify the concept of costumes for hospitality facilities of different regions, an analysis of the habitat species diversity of snakes was conducted. It shows that a wider species composition falls on the zones of the steppe and the mountain steppe – 6 species of snakes, forest-steppe and forest zone – 2 species, in the mountain forests – 3 species, and 3 types of snakes choosing areas near water.

However, under such wide variety of species, as graphic analysis shows, it is possible to allocate only five kinds of forms of a snake scales: rhombus, rhombus-stretched, rhombus with an overlay of scales one by one, hexagon, close to rhombus, and almonds (Figure 1).

It was revealed that most often on the snake's skin found diamond-like scales, living on the territory of Ukraine.

Flakes of snake skin combine into original mesh ornaments, which create harmonious relief-texture composite structures. All of these natural ornaments of the Slavic snake's skin can be used as an inspiration in textile design, and in designing clothes. Rhythmical and proportional patterns of snake's ornamentation when broadcast in the costume structure will allow organize its division and arrange compositional accents. Besides, an additional source of information for a costume designer, which uses Slavic serpents as inspiration in his creative activity, is a color pattern. The latter not only gives the desired color preferences, but also reveals the dominant ornamental accent within the mesh structure. In general, seven types of species of snake skin can identified of this region (Figure 1).

Ingredients of colored pattern of snake skin by layout structure are linear with mirror symmetry or displacement symmetry. Therefore, according to the analysis, which was carried out, can be argue that the patterns are based on a static or balanced asymmetric composition. That is, when designing costumes for the hospitality establishment's staff based on Slavic snakes ornamentation it is advisable to give priority to a vertically symmetric division or enter a small balanced asymmetry.

By the size and plasticity of contour lines, the character of the shaping elements of the ornament is nuancable. In the vast majority of ornaments leather cover of 11 types of snakes, living on the Ukraine territory, there are zigzag elements of the pattern and spots. Sometimes – strips and almost no monochrome scales, which can be also see in Figure 1.

As for the plastic of the elements contours of the snakes skin ornament, which investigated in this paper, can singled out as a leading straight-laced, aggressive.

However, sometimes there are elements of curvilinear form with less aggressive plastic.

In developing models of clothes on any subject, it is very important to analyze analog-models, but such analysis takes a lot of time.

Therefore, the development of recommendations is a very relevant and necessary task. Already ready basis will significantly simplify and accelerate the process of developing clothing, and in some cases inspire a designer and a costume designer.

Extension of the search and adaptation (read-only) series of perception the image of Slavic snakes in a suit is achieved by the recombination of the form elements, interacting with each other and nature of their combinations. Thus, the system integrity of the projected images is created. The basis of which is the layout material-form-design.

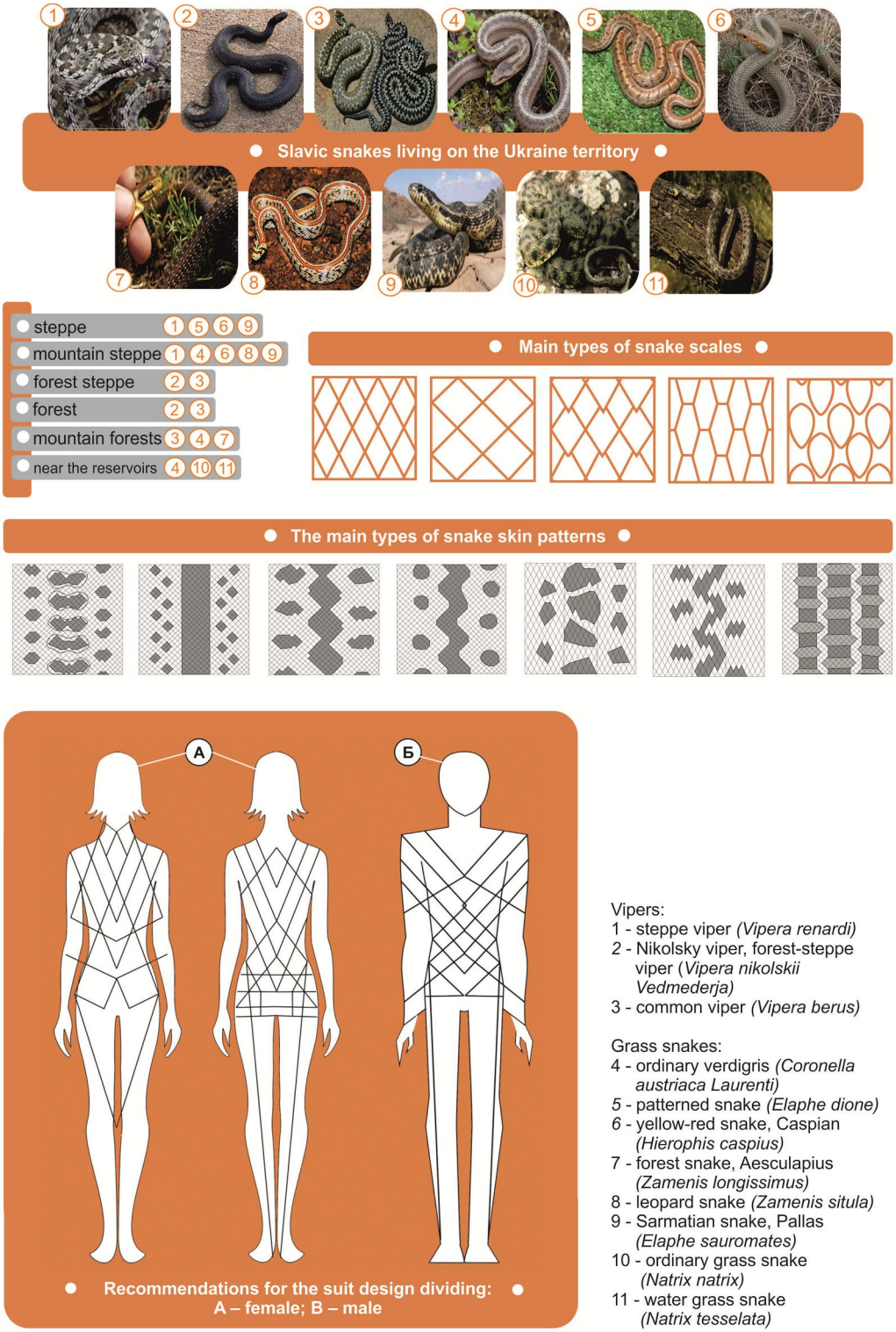

Figure 1 Analysis scheme of snake skin patterns

To facilitate structured search forms of suit-images of Slavic snakes the following recommendations for the principles of constructing their compositions were developed:

- The plastic form of the body of Slavic snakes built on smooth lines. In a suit, this can be achieved emphasizing the natural bends of the human body or, on the contrary, adding unnatural volume and convexity to the human body.
- A plastic contour element of the snake ornament, on the contrary, is mostly straight-laced, aggressive. Very rarely, there are elements of curvilinear form with less aggressive plastic. Such aggressive plastic is appropriate to use as small pieces of form or decorative elements.
- For snakes, characteristic horizontal and diagonal form splits. They are concentrated on the body on the wings, which adds a form of integrity and subordinate secondary items to the main one. Therefore, in the suit they should be located on the person's body. The compositional structure organization of the primary image of Slavic snake in costume is recommended and shown in Figure 1.
- Composition's connections of form parts according to the analysis, as well as the proportions of the costume and its elements must be based on identity or contrast.
- The character of the shaping elements of the ornament is nuanced, both in size and in the plasticity of contour lines. It is possible to use zigzag pattern elements and spots, as well as stripes.
- Form suit should have the center of gravity – focus, which is determined by the concentration of dominant signs and the axis of symmetry. The focus should be on the human body. According to the layout structure of the elements, the suit is based on mirror symmetry or displacement symmetry. At the heart of the costume composition, which is projected based on kite's inspiration, should lay static or balanced asymmetric composition.
- Rhythmic form organization based on metric ranks is created by scales, diamond-shaped or close to diamond-shaped shape and also horizontal or vertical stripes.

Figure 2 Graphic project of implementation the obtained research results

3 RESULTS AND DISCUSSION

As an illustration of the implementation process of the proposed recommendations in the design of clothing developed design-proposal for men's and women's costumes for waiters who work in hospitality establishments. They are conceptually focused on identifying regional peculiarities in their activities.

Figure 2 shows technical drawings the elements of both costumes and also their sketches in color on a person's figure. In sketches and technical drawings, we can clearly see the principle of applying the scheme of proposal suit division. It was built on the basis of analysis of Slavic snake's leather ornamentation. The use of characteristic ornamental structures of snake scales is proposed to be introduced into the decorative distinction of a suit. This is accomplished by drawing a simple geometric pattern by printing, machine embroidery or applique.

4 CONCLUSION

Therefore, research of leather ornamentation of Slavic snakes through graphical analysis picture populations of snakes, living in the territory of modern Ukraine, conducted in the article. Developed recommendations for the principles of constructing the Slavic snakes compositions in designing a women's and men's suit. Developed design- suggestions for men's and women's costumes for waiters who work in hospitality establishments. It allowed investigating that they are conceptually focused on identifying regional peculiarities in their activities.

5 REFERENCES

1. Sarobol A.: Costume development model for tourism promotion in Mae Hong Son province, Thailand, SHS Web of Conferences, Proceedings of 4th International Conference of Tourism Research (4ISTR), 12, 2014, 6 p., http://dx.doi.org/10.1051/shsconf/20141201053
2. Ya Nan He, Lin Zhang: Analyze on the tourism value of traditional costume culture resources in south jiangsu district and the development of tourism products, Advanced Materials Research 821-822, 2013, pp. 803-806, doi://10.4028/www.scientific.net/AMR.821-822.803
3. Yakymchuk O.V., Holubieva A.O.: Features of shaping the modern avant-garde costume, Arcadia. Art Studies and Culturological Magazine 2, 2015, pp. 95-99
4. Yakymchuk O.V.: Visual component of filmed image of Baba-Yaga, Herald of Kharkiv State Academy of Design and Arts 7, 2015, pp. 143-150
5. Yakymchuk O.V., Artemenko M.P., Phephelov A.O.: Visual component of filmed image of Koshchii Immortal, Herald of Kharkiv State Academy of Design and Arts 8, 2015, pp. 59-66
6. Semenenko Y.I., Yakymchuk O.V.: Problems of research images of Slavic myths. Scientific developments of youth at the present stage, Proceedigns of XIII th All Ukrainian Conference of Young Scientists and Students 2, 2014, pp. 404-405
7. Semenenko Y.I., Yakymchuk O.V.: Modern technologies of imitation of snake skin. Youth - science and production. Proceedigns of scientific and practical conference of students, 2014, pp. 18-19
8. Semenenko Y.I., Yakymchuk O.V.: Coloristic analysis and ornamental-texture component of images of Slavic snakes. Youth in the world of modern technology, Proceedings of III rd International scientific and practical conference of students, postgraduates and young scientists, 2014, pp. 105-110
9. Yakymchuk D.M.: Dynamics and development perspectives of Ukraine hotel and restaurant business. Modern directions of theoretical and applied research '2012, Collection of scientific works SWorld 1(2), 2012, pp. 73-76
10. Yakymchuk D.M., Yakymchuk O.V., Myrhorodska N.V.: Innovative feminine Indian suit as an inspiration of clothes design of hospitality establishments. Science and Education a New Dimension, Humanities and Social Sciences 139, 2017, pp. 7-9
11. Yakymchuk D., Yakymchuk O., Chepeliuk O. et al.: Study of cutting presses in designing a women's costume for hospitality industry, Eastern-European Journal of Enterprise Technologies. Engineering technological system 5(89), 2017, pp. 26-36, doi: 10.15587/1729-4061.2017.110962

HYDROPHOBIC ANALYSIS OF NANO-FILAMENT POLYESTER FABRIC

Musaddaq Azeem, Jakub Wiener and Muhammad Zaman Khan

Faculty of Textile Engineering, Technical University of Liberec, Studentská 1402/2, 461 17 Liberec 1, Czech Republic
musaddaqazeem@yahoo.com

***Abstract**: The aim of this study was to analyze the effect of hydrophobic finish for nano-filament polyester fabric with comparison to hydrophobic finish effect to cotton and Coolmax on the water transport property. nano-filament polyester, cotton and Coolmax fabrics were treated with 1% to 4% solution of hydrophobic finish (ItoguardLJ 100 conc.) to impart hydrophobicity. Hydrophobic behavior of theses fabric samples were measured by contact angle and roll off angle. Air permeability of treated and untreated fabric samples were compared regarding finish percentage applied. The results were as followed. The measured contact angle of water droplet on all fabric samples was 125-135° for 1-4% finish application. The tilting angles of all the samples were 11-18°. The air permeability values were inversely proportional to the finished percentage treatment. The best results were obtained at 3% finish applied on the fabric samples regarding contact angle, roll off angle and air permeability.*

***Keywords:** Nano-filament polyester fabrics, contact angle, roll of angle, air permeability.*

1 INTRODUCTION

Hydrophobicity with contact angles (CA) more than 90º are inspired by natural surfaces such as the lotus leaf, on which water drops show spherical shape and start roll off, removing dirt and dust substances from the surface [1]. Literature has given that hydrophobicity and superhydrophobicity prospective because of the mutual effect of hierarchical micro and nanostructures of the surfaces along with the low surface energy of the materials [2]. Hence, hydrophobic surfaces can be produced by creating roughness or by lowering the surface energy of a rough material. In textile industry, water proofing is considered as one of the likely applications for the superhydrophobic effect.

Superhydrophobic textiles are mostly applicable where textile surfaces are introduced to the environment [3, 4]. Different techniques have been applied to fabricate superhydrophobic fiber and textiles in a different ways as varied as electrospinning, sol-gel, plasma polymerization and surface coating [5, 6].

Polyester fiber has acquired 70% of textile fibre industry that is a significant figure. Although, it is known by its hydrophobic (low moisture regain) and electrostatic nature. To obtain better moisture transport, researchers think about modified polyester, especially with using multifilament and fine filament yarns. Multifilament polyester yarns are made by aggregating many continuous filaments together. They are characterized by their high strength, good chemical properties, acceptable elasticity and its circular cross section. Moreover, the voids between these filaments form capillary channels and facilitate liquid flow [7].

Nowadays we talk about ultrafine filaments or nano-filaments of polyester with diameters in the range of a few nanometers and lengths up to kilometers are used in different range of important technological applications such as functional fabrics, biomedicine, composite, etc. The nano-filaments of polyester are characterized by their high tenacity, large surface area per unit mass and small pore size [8].

2 MATERIALS AND METHODS

2.1 Material

Nano-filament samples were got from a Japanese commercial factory to asses it hydrophilicity and hydrophobicity properties for next to skin fabric. Yarn specifications for nano-filament polyester fabric are given in Table 1 followed by fabric specification Table 2.

Table 1 Mechanical properties of yarn used for the nano-filament fabric

Fineness	**[dtex]**	152±10
Tenacity	**[N]**	4.5±0.3
Elongation at break	**[%]**	32±5
Boil Shrinkage	**[%]**	2±1

Two samples were constructed by this yarn with different GSM. Both samples were fabricated by warp knitted technique and specifications are given in Table 2.

Table 2 Specifications of nano-filament fabric

Sample	GSM [g/m^2]	Thickness [mm]
S1	200±2	0.44
S2	250±2	0.55

SEM images are given below in Figure 1 to show the nano-filaments in yarn used for both sample construction.

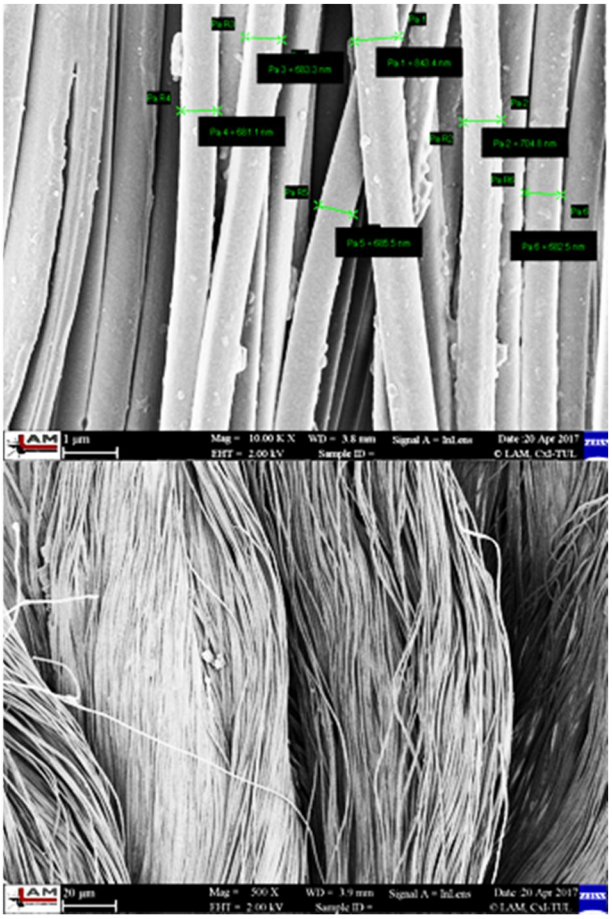

Figure 1 Fabric sample's SEM images with almost 680 nano-meter diameter

Sample 1 and sample 2 were compared with S3 (Coolmax) and S4 (cotton) fabric taken from university laboratory stock.

Table 3 Specifications of Coolmax and cotton

Sample	GSM [g/m^2]	Thickness [mm]	Yarn diameter [mm]	Yarn count
S3 (100% Coolmax)	200±2	0.69	0.12	20/1
S4 (100% cotton)	200±2	0.62	0.15	20/1

2.2 Methods

Lab scale method was used to make the solution of hydrophobic finish for treatment. 10, 30, 40 gram/liter Itoguard LJ 100 conc. finish solution with 2 drops of CH3COOH (conc.) applied onto the fabric samples to get hydrophobic properties [9, 10]. After immersion, samples were dried in the oven at 100°C for 15 minutes. Lastly, contact angle was measure on the fabric samples with contact Goniometry instrument [11]. For the measurement of roll-off angle, manual method was used as shown in Figure 2. The surface wettability of the treated nano-filament fabrics was studied by measuring the contact angle and roll-off angle of a droplet of water on their surfaces. Figure presents the profile of the instrument with both static and tilt position (droplet size, 10 µL).

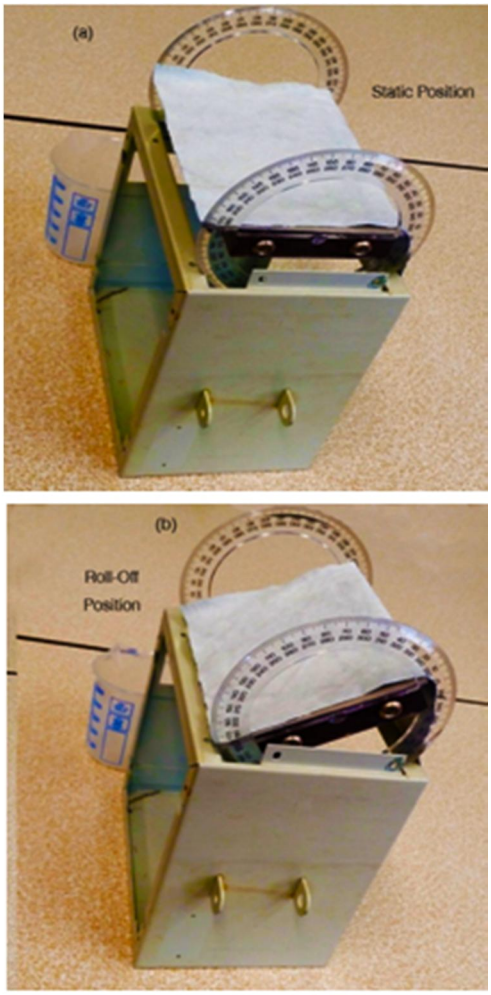

Figure 2 Roll-off angle instrument

Nano-filament polyester fabrics are more water lover as compared to PET spun fabric [8].

To analyze the water transportation of water through fabric samples, in house vertical wicking method was used with Czech standard (Czech national ČSN 80 08 28) was used, as shown in Figure 3. Coolmax and cotton fabrics (200 GSM) were also hanged on the instrument for the comparative results. Sample size was 250x10 mm. Ink drop was put into

the reservoir to clear the height of water on the fabric hanged vertically for results.

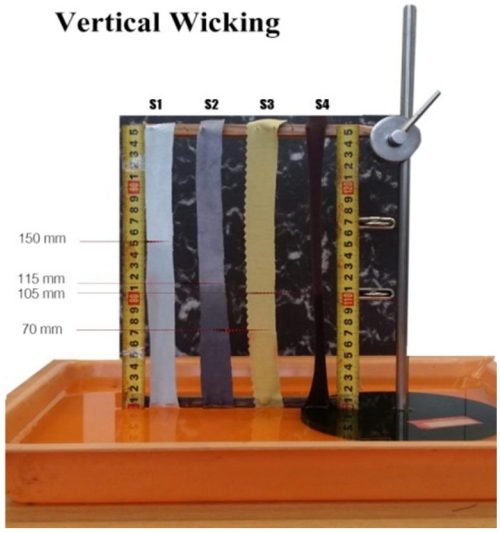

Figure 3 Vertical wicking method

Air permeability (ISO: 9237) SDL M021S method was used as shown in Figure 4. This test shows the level of resistance of the material to the air/wind influence from the outside. The lower permeability of the material the better is its resistance to air/wind.

Figure 4 Air permeability SDL M021S

3 RESULTS AND DISCUSSION

3.1 Vertical wicking

Water absorption and transportation of textiles is important for the optimization of underwear, functional clothing or other health-care products. Properties like vertical wicking should be investigating [12, 13]. Nano-filament fabric S1 with low mass showed better vertical wicking because of it less density. Tight structure of S2 restricted the filament to propagate the water. Coolmax and cotton fabric with porous material remained poorer in vertical wicking behavior as shown in Figure 5.

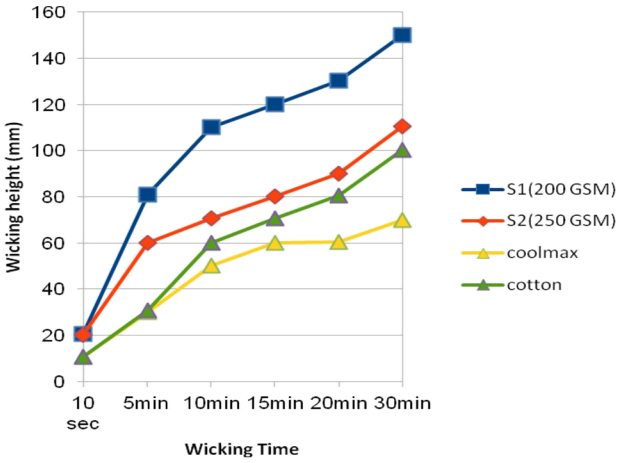

Figure 5 Vertical wicking

3.2 Contact Angle

Water contact angles were measured on Contact goniometry analysis system to determine the wettability of a surface [14, 15]. After applying the finishes when the samples were brought into contact angle measurement the observed contact angle of a water droplet on all fabric samples were 125-135°, for 1-4% finish applied. Graphical representation is showing no significant difference from 2% to 3% finish solution but compared to the 1% as shown below in Figure 6. Hydrophobic treatment with 3% finish is convenient and environmental process because of less use of finish quantity. The results shown in graph were not giving improved results by enhancing the percentage of finish in solution so 3% were found best for this process.

3.3 Roll-off Angle

The droplet roll-off state, because of the small total contact area between the liquid droplet and the surface [15, 16], is inversely proportional to the wettability. The tilting angles of all sample lie between 11-18°, the water droplet started to roll off the fabric surface. In comparison, figure below presents the profile of water droplets on a hydrophilic face. 4% finish solution onto the fabric sample exhibit better roll off angle other than 1-3% as sown in Figure 7.

3.4 Air Permeability

Air permeability of untreated and finished samples (1-4%) were measured by followed formula

$$R = \frac{q_r}{A} \times 10 \qquad (1)$$

Area of the diaphragm where fabric has to place is 20 cm. It was not found any significant difference when the samples were subjected to finish. But the air permeability of untreated fabric was slightly higher than treated fabric as shown in Figure 8.

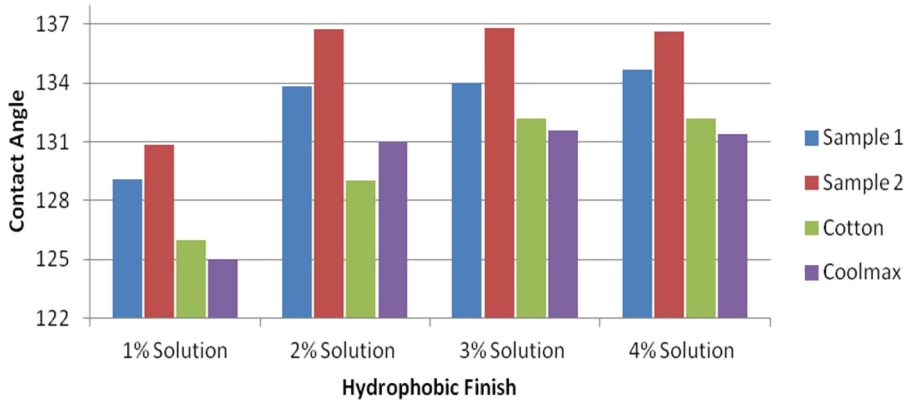

Figure 6 Contact angle measurement

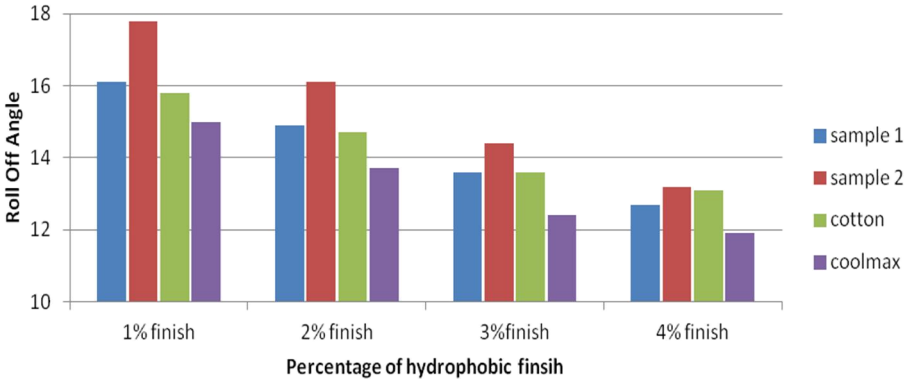

Figure 7 Roll off angle

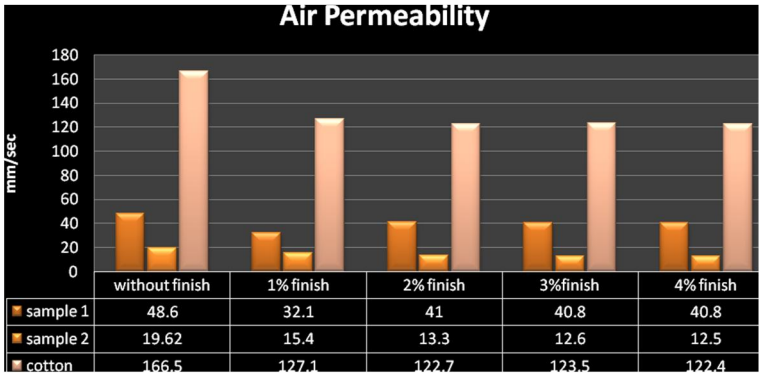

Figure 8 Air permeability index

4 CONCLUSIONS

From the obtained results it is concluded that the application of hydrophobic treatment to nano-filament polyester fabric along with cotton and multichannel fabric is also a promising textile finishing process to produce water repellent surface. In fact high contact angle and roll-off angle values were observed on all treated fabric sample without differentiate the structure and properties of specimens. The quantity of finish applied (%) was considered a significant parameter as compared to varying the fabric sample. The deposition of the hydrophobic finish on samples was 1 to 4%. Moreover, 3% finish applied was enough to confer the desired results. The air permeability values were found inversely proportional to the hydrophobic finished percentage treatment.

ACKNOWLEDGEMENTS: *The authors would like to thank the Technical University of Liberec (TUL) for Student Grant (SGS 21247) 2018.*

5 REFERENCES

1. Li X., Reinhoudt D., Crego-Calama M.: What do we need for a superhydrophobic surface? A review on the recent progress in the preparation of superhydrophobic surfaces, Chemical Society Reviews 36, 2007, pp. 1350-1368
2. Patankar NA.: Mimicking the lotus effect: influence of double roughness structures and slender pillars, Langmuir 20, 2004, pp. 8209-8213
3. Zhang B.T., Liu B.L., Deng X.B., Cao S.S., Hou X.H., Chen H.L.: Fabricating superhydrophobic surfaces by molecular accumulation of polysiloxane on the wool textile finishing, Colloid and Polymer Science 286, 2008, pp. 453-457
4. Pan C., Shena L., Shang S., Xing Y.: Preparation of superhydrophobic and UV blocking cotton fabric via sol–gel method and self-assembly, Applied Surface Science 259, 2012, pp. 110-117
5. Xu B., Cai Z.: Fabrication of a superhydrophobic ZnO nanorod array film on cotton fabrics via a wet chemical route and hydrophobic modification, Applied Surface Science 254, 2008, pp. 5899-5904
6. Ji Y.Y., Hong Y.C., Lee S.H, Kim S.D., Kim S.S.: Formation of super-hydrophobic and water-repellency surface with hexamethyldisiloxane (HMDSO) coating on polyethyleneteraphtalate fiber by atmospheric pressure plasma polymerization, Surface Coating Technology 202(22-23), 2008, pp. 5663-5667
7. Sampath M.B., Mani S., Nalankilli G.: Effect of filament fineness on comfort characteristics of moisture management finished polyester knitted fabrics, Journal of Industrial Textile 41(2), 2011, pp. 160-173
8. Chronakis I.S.: Micro-/nano-fibers by electrospinning technology: processing, properties and applications. Micromanufacturing Engineering and Technology, Boston: Elsevier 2010, pp. 264-286
9. Zaman M., Liu H., Xiao H., Chibante F., Ni Y.: Hydrophilic modification of polyester fabric by applying nanocrystalline cellulose containing surface finish, Carbohydrate Polymers 91, 2013, pp. 560-567
10. Dave J., Kumar R., Srivastava HC.: Studies on modification of polyester fabrics I: Alkaline hydrolysis. *Journal of Applied Polymer Science* 1987, 33, pp. 455–477.
11. Kabza K.G., Gestwicki J.E., McGrath J.L.: Contact angle goniometry as a tool for surface tension measurements of solids, using Zisman Plot method. A physical chemistry experiment, Journal of Chemical Education 77(1), 2000, pp. 63-68
12. Harnett .PR., Mehta P.N.: A survey and comparison of laboratory test methods for measuring wicking, Textile Research Journal 54, 1984, pp. 471-478
13. Wiener J., Dejlová P.: Wicking and wetting in textiles, AUTEX Research Journal 3, 2003, pp. 64-71
14. Stanssens D., Abbeele H.V., Vonck L., Schoukens G., Deconinck M., Samyn P.: Creating water-repellent and super-hydrophobic cellulose substrates by deposition of organic nanoparticles, Materials Letters 65, 2011, pp. 1781-1784
15. Zhou X., Zhang Z., Xu X., Men X., Zhu X.: Fabrication of super-repellent cotton textiles with rapid reversible wettability switching of diverse liquids, Applied Surface Science 276, 2013, pp. 571-577
16. Bagherzadeh R., Montazer R., Latifi M., Sheikhzadeh M., Sattari M.: Evaluation of comfort properties of polyester knitted spacer fabrics finished with water repellent and antimicrobial agents, Fibers and Polymers 8(4), 2007, pp. 386-392

EXPERIMENTAL STUDY OF GLUING AS A JOINING METHOD FOR GARMENTS

Erdal Ekinci, Irina Nowikowa and Andrea Ehrmann

Bielefeld University of Applied Sciences, Faculty of Engineering and Mathematics, 33619 Bielefeld, Germany
andrea.ehrmann@fh-bielefeld.de

Abstract: *Seams of garments and other textile fabrics are usually sewn. Different adhesive techniques can be used to connect textile materials for special purposes, often to create waterproof seams. Gluing and other bonding methods, however, usually necessitate special machines which are not always available in textile production companies. On the other hand, only few reports about using household adhesives can be found in the literature. This is why this paper reports on tests of different commercially available adhesives which were used to bond diverse textile fabrics. The results show that most of these adhesives are not suitable for creating reliable bonds between most textile materials. Only one of the two-component adhesives under examination which is flexible, but not explicitly suggested for textile fabrics has shown to create sufficient adhesion forces between most textile materials.*

Keywords: *gluing, bonding, seam strength, adhesion.*

1 INTRODUCTION

Sewing is the most commonly used joining technique for textile fabrics. Nevertheless, other bonding methods are already available, from ultrasonic welding to laser welding to gluing. All these technologies have the advantage that they can be automatized.

For smaller textile companies, however, the necessary machines are often not affordable. Even simple adhesive bonding techniques often necessitates special machines. Additionally, gluing of textile material has not often been described in the literature.

One area in which adhesives are often used in combination with textile materials is adding textile RFID tags to garments or other fabrics. Since the tag IC often cannot be sewn to create a connection with the textile antenna, it is glued instead. In a recent article, e.g., the RFID chip was connected with the antenna via embroidery with conductive yarn or conductive glue [1]. Adhesives were also used to cover RFID tags consisting of an antenna from brush-painted silver ink with common IC chip and thus protect them during washing [2], finding that the textile glue showed better shielding performance than epoxy or silicone rubber coatings [3]. Glue-type coatings on RFID tags on textile fabrics were found to be easier to handle and to spread than others, with harder coatings sometimes being preferable due to their ability to prevent the conduction lines from breaking [4]. Similar results were found for a comparison of textile antennas produced by patterning silver-plated fabrics and brush-painting silver ink on cotton fabrics, where the latter showed better results after 10 washing cycles [5].

Few approaches have been made to investigate the use of textile adhesives for bonding instead of coating. Aluminium foils, e.g., were glued on basalt fiber fabrics to create personal protective equipment against thermal and mechanical impacts [6]. Textile-wood composites were created and examined with respect to their mechanical properties, using natural bone glue and a polyvinyl adhesive [7].

Similarly, basalt, lavsan and blended fabrics were glued with a PVC film to create composites with high mechanical and flame-proof properties [8]. Layered fabrics consisting of textile fabrics and membranes were also constructed using adhesives, modifying the diffusion coefficient by diverse treatments [9].

Nevertheless, while the influence of sewing parameters on the seam strength is sometimes investigated for special applications [10, 11], similar investigations cannot be found in scientific literature for glued bonds between textile fabrics. Only the adhesion forces between small electronic elements and diverse textile materials were investigated yet [12, 13].

This article thus gives a first overview of the broad spectrum of adhesion forces which can be reached using different combinations of textile fabrics and nontoxic adhesives which can be applied without machines.

2 EXPERIMENTAL

The textile fabrics used in this examination are depicted in Table 1. The chosen materials are typical for garment construction.

Table 1 Textile fabrics used for the tests

Fabric material	Construction	Areal weight [g/m²]
100% cotton (CO)	Woven	120
100% polyester (PES)	Woven	170
100% linen (LI)	Woven	245
95% CO, 5% elastane (EL)	Knitted	217
95% PES, 5% EL	Knitted	180
65% PES, 35% CO	Woven	105

Three commercially available household adhesives were used and compared with nontoxic, easily applicable industrial adhesive and the force gained by sewing. All adhesives are elastic and specified as water-resistant. The following products were used: textile glue (Bindulin), all-purpose glue (UHU), two-component adhesive (Bindulin), and the industrial glue DELO-DUOPOX® 02 rapid (Delo). The adhesives were applied on the textile fabrics using a doctor's knife and dried according to the respective instructions (Figure 1); the samples with textile adhesive were afterwards ironed at a temperature range of 130-165°C.

For sewing, 100% polyester yarn Ne 40/2 was used in a sewing machine Victoria / model 785 with a single universal needle 80/12, using a double lockstitch with a stitch length of 3 mm. One seam was applied in the middle of the sample.

Five samples of each combination were prepared and tested according to DIN 53530; the results were evaluated according to DIN ISO 6133. Since the sample width is 25 mm, the measured adhesion forces are scaled to a width of 1 cm in the results. No scaling was performed for the sewn samples. This means that in the results, glued seams of 1 cm width are compared with sewn connections of significantly smaller width, which has to be taken into account in the evaluation of the results.

Measurements were performed using a Sauter universal testing machine. For washing tests, a washing machine Bosch Maxx was used, applying heavy-duty detergent (Tandil, 20 ml) and softener (20 ml) during one washing cycle at 30°C for 1.5 h and a spin cycle with 1400 min^{-1}. Washing was followed by subjective evaluation of the samples.

3 RESULTS AND DISCUSSION

Figure 1 depicts a sample series during drying. As visible here, some adhesives were hard to spread regularly on the samples, depending on their viscosity, partly resulting in non-uniformly glued samples.

Figure 1 Textile strips, glued with different adhesives, drying at room temperature

The effect of this problem is visible in Figure 2. Here, both samples with higher adhesion start with nearly exactly identical values. The irregularly glued sample, however, shows significant decreases in the adhesion force, finally resulting in a reduced average adhesion, as evaluated according to DIN ISO 6133. This effect must be kept in mind for possible applications in small companies – adhesives which cannot be applied regularly with typical textile technologies, such as a doctor's knife, are not suited for these purposes.

On the other hand, the blue curve shows a significantly smaller adhesion force. This combination of adhesive and textile material is apparently not suited for industrial application, either.

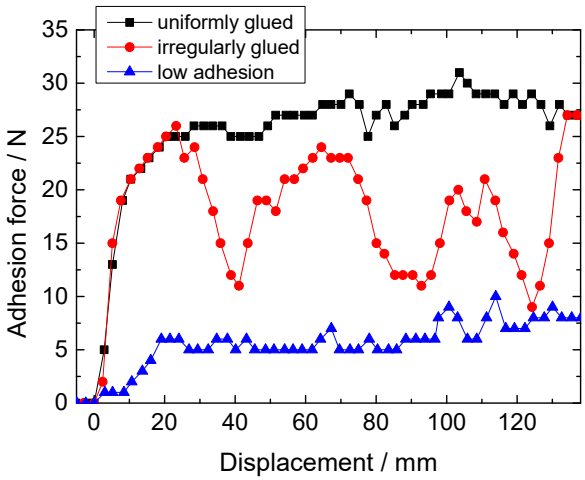

Figure 2 Typical force-displacement curves for different glued samples, either glued uniformly with a high adhesion, irregularly – but with a high adhesion at some positions –, or with a constantly low adhesion

A comparison of the adhesion forces of all material combinations under investigation is depicted in Figure 3. It should be mentioned that for sewing, the absolute force [N] is given, as described above.

Firstly, the all-purpose glue shows low adhesion forces on most textile materials and is thus not suited for gluing textiles. Additionally, the large error bars indicate severe irregularities in the adhesive application. The two-component glue shows similarly

low adhesion, on CO and CO/EL near to zero. Interestingly, the bonds created by the textile glue are not much stronger. This finding is in agreement with former experiments gluing electronic parts on textile fabrics [12, 13].

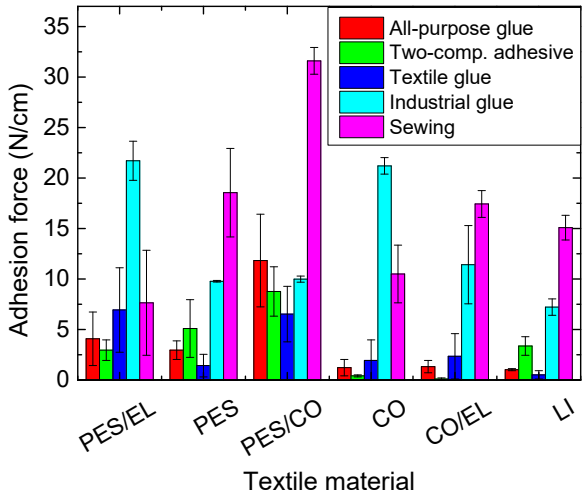

Figure 3 Adhesion forces for diverse combinations of textile materials and adhesives

Sewing leads to adequate seam strengths in all cases, usually with the highest values of all bonds. Nevertheless, the industrial glue gives sufficient adhesion values on all textile materials except PES/CO. The large error bar found for industrial glue on CO/EL results from the textile fabric being destroyed during the tests, without the adhesive being detached. This shows that gluing instead of sewing is principally possible, while nevertheless this decision must be made separately for each material combination.

Finally, it must be mentioned that in this test, a glued seam of 10 mm width is compared with a sewn seam of less than 1 mm width. Although all adhesives are elastic, such a broad seam will definitely modify the bending stiffness and the haptics of a garment or another textile fabric. Even with the industrial glue, unremarkably thin seams are not yet possible.

The results of the washing tests are given in Table 2, with a scale from + (no modifications) to 0 (small modifications) to – (strong or complete delamination).

Interestingly, while the industrial glue and sewing work with all fabric materials, no general trend is visible for the household glues. Apparently, all of the adhesives work well with some materials and have lower adhesion on others. This means that none of the household glues tested here can be used for all textile materials.

Additionally, the best combinations in the washing tests do not correspond to the ideal combinations in the adhesion tests. None of the household glues is thus suitable for producing reliable, washable bonds between textile materials.

Table 2 Results of washing experiments

Fabric material	All-purp.	2-comp.	Textile	Indust.	Sew.
CO	0	0	0	+	+
PES	+	-	0	+	+
LI	+	0	-	+	+
CO/EL	0	-	+	+	+
PES/EL	+	-	-	+	+
PES/CO	0	+	-	+	+

4 CONCLUSION

To conclude, we have compared the adhesion forces of different adhesives and a sewn seam combined with diverse textile materials which are typical for garment production. While sewing and the industrial glue work sufficiently in adhesion and washing tests, the household glues suffer from low adhesion in at least one of the tests.

Future experiments will thus concentrate on testing further flexible industrial glues and increasing the uniformity of the adhesive application with equipment typically available in the textile industry, such as doctor knives or roller squeegees.

***ACKNOWLEDGEMENT**: The authors would like to thank DELO Industrie Klebstoffe (Windach / Germany) for providing samples of diverse two-component adhesives.*

5 REFERENCES

1. Shuaib D., Ukkonen L., Virkki J., et al.: The possibilities of embroidered passive UHF RFID textile tags as wearable moisture sensors, IEEE International Conference on Serious Games and Applications for Health 2017, 5
2. Fu Y.Y., Chan Y.L., Yang M.H., et al.: Experimental study on the washing durability of electro-textile UHF RFID tags, IEEE Antennas and Wireless Propagation Letters 14, 2015, pp. 466-469
3. Kazmi A., Rizwan M., Sydanheimo L., et al.: A reliability study of coating materials for brush-painted washable textile RFID tags, In 6th Electronic System-Integration Technology Conference (ESTC), 2016
4. Kellomaki T., Virkki J., Merilampi S., et al.: Towards washable wearable antennas: A Comparison of coating materials for screen-printed textile-based UHF RFID tags, International Journal of Antennas and Propagation 2012, 2012, no. 476570
5. Kazmi A., Virkki J., Bjorninen T., et al.: Performance of silver-based textile UHF passive RFID tags after recurrent washing, IEEE Antennas and Propagation Society International Symposium 2016, 2016, pp. 939-940
6. Hrynyk R., Frydrych I., Irzmanska E., et al.: Thermal properties of aluminized and non-aluminized basalt fabrics, Textile Research Journal 83, 2013, pp. 1860-1872
7. Cosereanu C., Curtu I., Lunguleasa A., et al.: Influence of synthetic and natural fibers on the characteristics of wood-textile composites, Materiale Plastice 46, 2009, pp. 305-309

8. Morozova M.Y., Polushenko I.G.: Study of the possibility of creating complex textile material based on fibre blends, Fibre Chemistry 40, 2008 pp. 50-53
9. Fohr J.P., Couton D., Treguier G.: Dynamic heat and water transfer through layered fabrics, Textile Research Journal 72, 2002, pp. 1-12
10. Raj D.V.K., Devi M.R.: Performance analysis of the mechanical behaviour of seams with various sewing parameters for nylon canopy fabrics, International Journal of Clothing Science and Technology 29, 2017, pp. 470-482
11. Schwarz I.G., Kovacevic S., Kos I. Physical-mechanical properties of automotive textile materials, Journal of Industrial Textiles 45, 2015, pp. 323-337
12. Klöcker M., Ellouz M., Ehrmann A., et al.: Examination of commercially available fabric glues, Technical Textiles 58, 2015, p. E272
13. Klöcker M., Aumann S., Ellouz M., et al.: Effect of textile pre-treatments on electronics-textile glued connections, Proceedings of Aachen-Dresden International Textile Conference, 2015

THE OPTIMAL DOLOMITE PARTICLES SIZE ADDED TO THE ACRYLIC COATING OF BOOKBINDING CANVASES

Hana Křížová[1], Jitka Neoralová[2] and Jakub Wiener[1]

[1]Technical University of Liberec, Faculty of Textile Engineering, Department of Material Engineering, Studentská 2, Liberec, Czech Republic
[2]National Library of the Czech Republic, Development and Research Laboratories, Sodomkova 2, Prague, Czech Republic
hana.krizova@tul.cz, Jitka.Neoralova@nkp.cz, jakub.wiener@tul.cz

Abstract: *The aim of this research was to find the optimal size of the dolomite particles added to the acrylic coating for use on book canvas. To increase durability and resistance of archived books from acid environment, milled dolomite was used as an alkaline buffering agent. It was found that rough dolomite particles increase the surface roughness and worsen the mechanical properties of canvas, especially abrasion. However, they also most significantly alkalize and buffer the canvas surface in aqueous environment. The optimum size of the dolomite particles in the coating was achieved by balancing these properties.*

Keywords: *dolomite, canvas, coating, alkaline reserve, abrasion, roughness.*

1 INTRODUCTION

Books in archives and library collections are exposed to chemical [1], biological [2] and physical [3] effects. It leads to their damage during their archivation [4]. Due to these effects, we lose the valuable cultural heritage and knowledge recorded in the books. Repair of book bindings is very costly and labor intensive [5]. Additives in the coating may affect some properties of canvases, e.g., strength [6, 7], abrasion [8], resistance to insects and fungi [9], combustibility [10], etc. Due to environmental pollution, the air usually contains acid-generating oxides [1] (mainly sulphur dioxide) and a lot of inorganic and organic compounds. In the air of archives and libraries, volatile organic compounds such as benzene, toluene, ethylbenzene, xylenes or furfural which are a known marker of paper degradation are usually detected [11]. Alkaline reserve with buffering ability such as carbonates of alkaline earth metals (calcium carbonate, magnesium carbonate, calcium magnesium carbonate or dolomite) can also help to avoid a prolonged exposure to an acidic environment, which, in conjunction with moisture leads to acid hydrolysis. The consequence of acid hydrolysis of cellulose [12] is the loss of strength and decreased durability of paper and bookbinding canvas of archived books [13].

The fundamental challenge was to find the ideal size of the particles to be used as an additive to dual-layer acrylate coating. Too large particles of carbonate mineral worsen the look and touch feelings and increases surface abrasion of the canvas, which leads to its premature mechanical damage [14]. On the other hand, too small particles in the coating can be covered in large part by surrounding acrylate and may not exhibit sufficient activity in the surface contact of canvas with moisture and acid air. Since it is difficult to imitate the conditions in the archive, including effect of time [15], the simulation of negative factors of the environment was very simplified. We used milled and washed dolomite with different particle size (in range from hundreds of nanometers to tens of micrometers) as alkaline buffering additive [16] to the acrylate coating to create the bookbinding canvas with extended life. We examined the appearance and surface roughness of created canvases by image analysis. Subsequently, these samples were exposed to an aqueous environment where followed the changes in pH environment caused by the gradual release of dolomite over several days. Furthermore, we evaluated their buffering capacity in the gradual acidification by airy carbon dioxide. Finally, we concluded the optimal size of particles used in the coating regarding chemical and mechanical requirements of the developed book canvas.

2 EXPERIMENTAL PART

2.1 Material

Cotton fabric Sara (Licolor, CZ), area weight 135 g/m^2, fabric thickness 0.37 mm; Acronal S 996 S (BASF SE, GE) - aqueous polymer dispersion based on ester of acrylic acid and styrene, viscosity 2 Ns/m^2; granulated natural pink dolomite (anhydrous calcium magnesium carbonate, $CaMg(CO_3)_2$) for agricultural use (Forestina, CZ); TSA (Tryptic soy

agar) in Petri dishes (BioVendor, CZ); Martindale abrasive cloth SM 25 (James Heal, England), ISO 12947-1:1998 [17].

2.2 Methods and devices

Commercial pink dolomite for agricultural use was dosed into cartridges of ball mill with zirconia balls of 1 cm diameter. Ten milling cycles (each of 5 min) with cooling intervals was carried out at 800 rpm. The dolomite was subsequently separated using different speeds of sedimentation of the particles in a glass cylinder filled with water to four fractions with different particle sizes. The resulting particle size of dolomite was measured using the particle size analyzer and laser scattering device (HORIBA LA-920, JP).

Each fraction was added to Acronal in an amount of 3% by weight of the coating paste, mixed thoroughly and these homogenized mixtures were used for coating of cotton fabric. Canvases were prepared using a laboratory coating device. All canvases were coated with two layers of coating and then condensed at 140°C for 2 minutes and dried at 100°C for 15 minutes.

The surfaces of coated canvases were scanned using the 3D digital multifunction microscope HIROX RH 2000 (MXB 2500REZ lens, diffuse adapter). Surface roughness (Rz) measurement was provided in accordance with Japanese Industry Standard (JIS) B0601 (1994) [18]. Rz is the sum of the average absolute value of the height (five highest peaks) and the average absolute value of the depth (five lowest valleys from the average line of the roughness curve) on the weft yarn, in micrometers. Ten-spot average roughness was chosen at zoom 1000x.

Fifteen cm^2 of each canvas including the reference sample (cotton fabric coated with acrylic coating without dolomite) was immersed in 50 ml of purified deionized water for several days at 22±2°C and its pH changes were continuously potentiometrically measured using glass silver chloride reference electrode.

Bacteriological control of water purity was carried out by a simple test, when 1 ml of water from each sample was inoculated on the agar (TSA) in Petri dishes. It was incubated for 24 hours at 37°C and subsequently bacterial colonies (CFU) were counted.

The abrasion resistance of canvas surface was tested according to the standard ISO 5470-2: 2003 [19] using Martindale Abrasion and pilling tester device (James H. Heal and Co. Ltd. England). Four circular samples with a diameter of 37 mm from each canvas were clamped in holders of Martindale device together with the pad of foam material, each with a down pressure of 12 kPa. Face (coated) side of canvases has been tested with the speed of about 60 rpm. The testing was performed using special Martindale abrasive cloth. In accordance with the standard [19] the abrading face side of canvases was controlled and visually evaluated according to a standardized scale (grade 0-5) in the following checkpoints: 1600, 3200, 6400, 12800, 25600 and 51200 abrasive revolutions.

2.3 Results

Result of particle size measurement using device HORIBA LA-920 (Figure 1) shows that after ten milling cycles in nano mill with zirconia balls the particle size of dolomite ranged from about 0.5 to 50 μm.

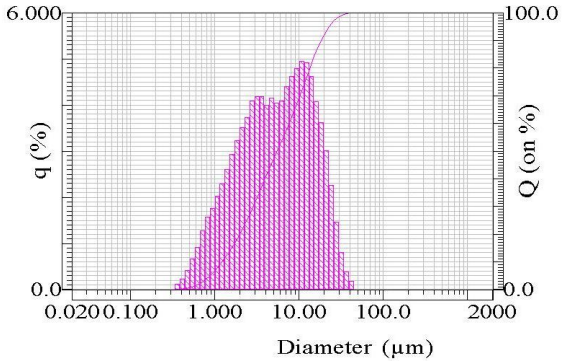

Figure 1 Distribution of dolomite particle sizes after 10 milling cycles in nano mill with zirconia balls

Figure 2 shows that particles of milled dolomite were sorted into 4 parts with the size of about 1 μm, a few micrometers and tens of micrometers based on the different sedimentation velocity of particles in the water column. These particles were used as an additive to the acrylic coating of cotton fabric, to give the four canvases with different roughness (Figure 3).

Table 1 Roughness of canvases No. 0-4 measured at magnification of 1000

	Canvas No.				
Rz JIS [μm]	**0**	**1**	**2**	**3**	**4**
Minimum	10.1	10.2	13.7	13.2	35.7
Maximum	10.8	17.5	21.5	27.8	39.0
Avarage	**10.44**	**14.48**	**17.12**	**24.2**	**37.14**
Median	10.4	16.9	14.8	26.9	36.6
S.d.	0.27	3.42	3.51	5.56	1.36

An overview of roughness coefficients (Table 1) confirmed the touch feeling of coating whose roughness increased with the addition of larger particles of dolomite.

Table 2 Abrasive properties of canvases No.0-4

Canvas No.	Grade of abrasion in the checkpoint					
	1600	***3200***	***6400***	***12800***	***25600***	***51200***
0	0	0	0	1	1	1
1	0	0	0	1	1	1
2	0	0	0	1	1	1
3	0	0	1	1-2	2	2
4	0	1	2	3	3-4	4

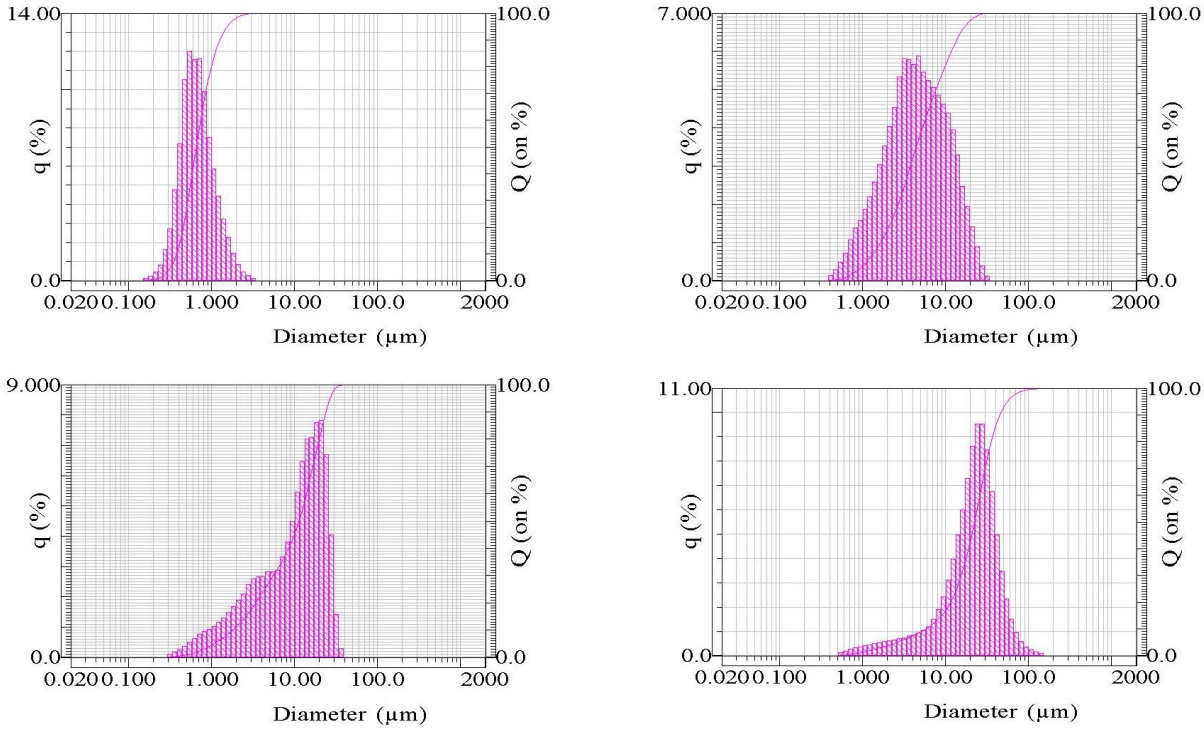

Figure 2 Four dolomite fractions sedimented in a glass cylinder with water during 1 to 24 hours. The average particle size: 0.75 (top left) – 6.20 (top right) – 12.30 (bottom left) – 48.60 µm (bottom right)

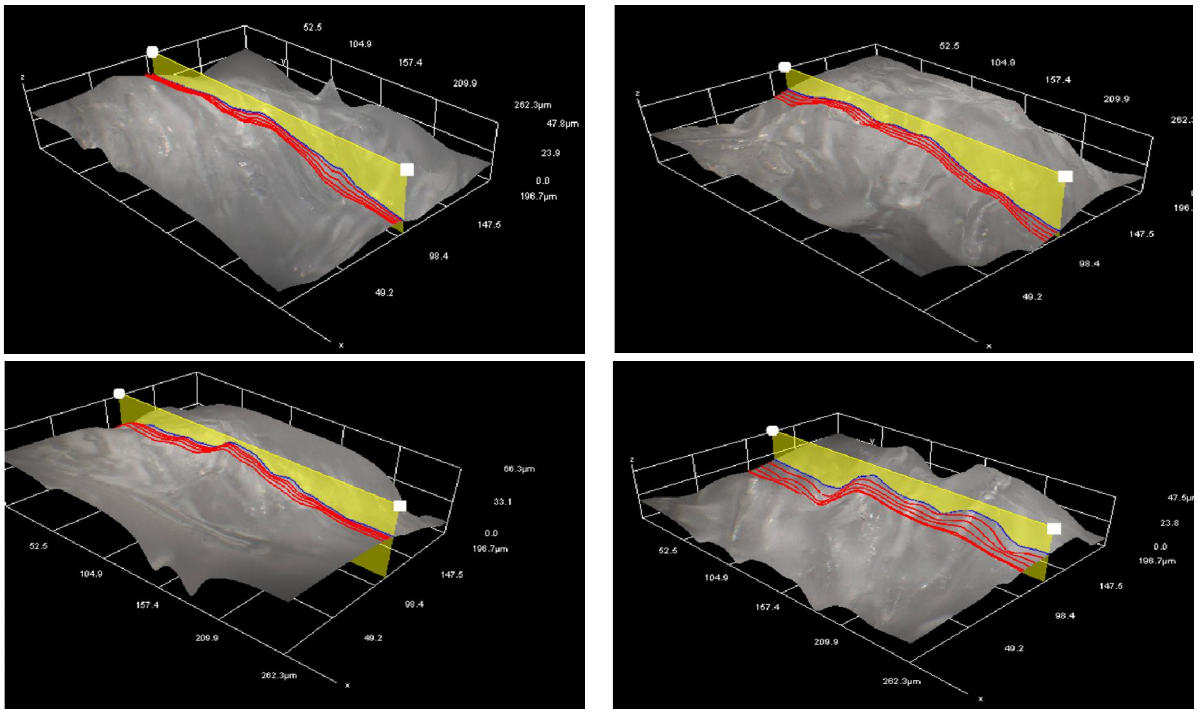

Figure 3 3D images of canvas surfaces: canvas No.1 (top left) – canvas No.2 (top right) – canvas No.3 (bottom left) – canvas No.4 (bottom right), zoom 1000x

Figure 4 shows the changes of pH in the water in which these canvases were inserted for 17 days. Fabrics with increasing particle size of dolomite in the coating were labeled No. 1-4. Canvas with acrylic coating without addition of dolomite is marked by zero, basic solution without canvas (purified water for injection) was marked by *A*.

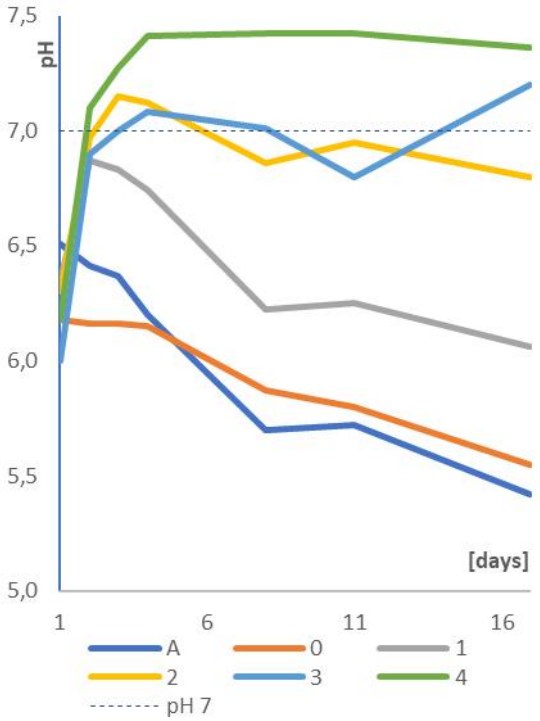

Figure 4 Changes of pH in aqueous solutions containing canvases with increasing particle size in the coating (1-4) for 17 days. Reference samples: 0 (canvas without dolomite in the coating), *A* (only water without canvas)

3 DISCUSSION

Different sedimentation rate of dolomite particles with different sizes and weight in the water column allowed their separation into four groups, with an average particle size of about 1, 6, 12 and 48 μm. Different roughness of canvases with coating containing these particles was distinguishable by the touch. Calculation based on 5 measurements of surfaces using 3D microscope differentiated these average roughness value from 10.44 to 37.14 μm. It is evident from Figure 4 that pH value in water samples containing canvases No. 1-4 increased in the early days. From about 4th day pH value in samples A, 0, 1 and 2 began decrease. Test of water bacteriological purity of all samples was conducted out the eighth and seventeenth day of the experiment. The suspicion that the pH value decreased due to bacteriological contamination was not confirmed (the number of grown bacteria was less than 5 CFU/1 ml). The cause of pH decrease in aqueous samples was therefore influence of atmospheric CO_2 (beakers with canvases immersed in water were not closed). Airy carbon dioxide dissolves slowly in water to form carbonic acid, which results in decrease of pH. As shown in Figure 4, pH of the sample 3 began to decrease slightly from the 8th day, the sample pH 4 from the 17th day. Samples No.3 and 4 (samples with the largest dolomite particles in the coating) alkalized and buffered the acidification caused by the influence of CO_2 for longer time and efficiently. This chemical process can be expressed by equations (1) and (2) [20]

$$CaCO_3 + CO_2 + H_2O = Ca(HCO_3)_2 \quad (1)$$

$$MgCO_3 + CO_2 + H_2O = Mg(HCO_3)_2 \quad (2)$$

As expected, abrasion tests on Martindale device showed that the canvas No. 4 with dolomite particle size of tens of micrometers in coating had the worst abrasion properties (Table 2). It achieved grade 4 (it means significant damage: the cover coating was broken and the middle layer was disturbed) at the last checkpoint. It is therefore unsuitable for use as a bookbinding canvas, because it would be very soon mechanically damaged and aesthetically unsightly (capture of dirt). Canvases No. 3, 2 and 1 however, exhibited good abrasion properties (grade 1-2, it means very slight to moderate damage with a change of gloss and no or only slight damage of the coating).

4 CONCLUSION

The aim of this research was to determine the optimum particle size of the powdered additive in the acrylic coating of canvas. The expected characteristics were alkalizing (buffering) ability in the moisture, and good mechanical properties, particularly an acceptable abrasion. We chose milled dolomite, whose particles had a size from several hundred of nanometers to several tens of micrometers. We added it into coating in concentration of 3 wt.% of the acrylic paste. We ascertained that the best properties of alkaline reserve met dolomite with particle size of tens of micrometers (canvas No. 4). However, this particle size also very worsened the canvas abrasion. Relatively good long-term buffering capacity was observed in canvas No. 2 with coating containing the dolomite fraction with particle diameter from 1 to 20 μm (average 6.2 μm, median 4.5 μm) and where 70% of particles ranged between 2 and 10 μm. This canvas maintained the pH of aqueous solution in the range from 6.9 to 7.15 for 17 days and met very good nonabrasive properties, because it reached grade 1 only (loss of gloss without damage) at the endpoint (51 200 rpm). We are convinced that the dolomite with particle size between 2 and 10 μm in 3% concentration is very suitable additive to the coating of bookbinding canvases with extended lifetime for archiving as well as borrowing mode.

***ACKNOWLEDGEMENT**: This work was supported by the project No. DF13P01OVV004 Exploration, conservation and care of modern library collections - materials and technologies provided by the Ministry of Culture within the Program of applied research and development of national and cultural identity (NAKI).*

5 REFERENCES

1. Blades N., Oreszczyn T., Bordass W., et al.: Guidelines on pollution control in museum buildings. Museum Practice, Museums Association, London 2000
2. Zyska B.: Fungi isolated from library materials: a review of the literature. International Biodeterioration & Biodegradation 40(1), 1997, pp. 43-51
3. Buchanan S.: Disaster, prevention, preparedness and action, Library trends 30(2), 1981, pp. 241-252.
4. Middleton B.C.: Book preservation for the librarian, Advances in Chemistry 164, 1977, pp. 3-23
5. Cockerell D.: Bookbinding, and the care of books, General Books, 2010
6. Křížová H., Wiener J.: Increase of cotton canvas strength by addition of nanocellulose to the coating, Proceedigns of 8th International Conference NANOCON, 2016, pp. 324-329
7. Azizi Samir M.A.S., Alloin F., Dufresne A.: Review of recent research into cellulosic whiskers, their properties and their application in nanocomposite field, Biomacromolecules 6(2), 2005, pp. 612-626
8. Wiemann M.: Canvas abrasive material and grinding process, U.S. Patent No. 6,482,308, 2002
9. Cioffi N., Torsi L., Ditaranto N., et al.: Copper nanoparticle/polymer composites with antifungal and bacteriostatic properties, Chemistry of Materials 17(21), 2005, pp. 5255-5262
10. Chapple S., Anandjiwala R.: Flammability of natural fiber-reinforced composites and strategies for fire retardancy: a review, Journal of Thermoplastic Composite Materials 23(6), 2010, pp. 871-893
11. Cincinelli A., Martellini T., Amore A., et al.: Measurement of volatile organic compounds (VOCs) in libraries and archives in Florence (Italy), Science of the Total Environment 572, 2016, pp. 333-339
12. Fan L.T., Gharpuray M.M., Lee Y.H.: Acid hydrolysis of cellulose, In: Cellulose Hydrolysis, Springer Berlin Heidelberg, 1987, pp. 121-148
13. Smith R.D.: Paper deacidification: a preliminary report, The Library Quarterly 36(4), 1966, pp. 273-292
14. Backer S., Tanenhaus S.J.: The relationship between the structural geometry of a textile fabric and its physical properties: Part III: Textile geometry and abrasion-resistance, Textile Research Journal 21(9), 1951, pp. 635-654
15. Area M.C., Cheradame H.: Paper aging and degradation: recent findings and research methods, BioResources 6(4), 2011, pp. 5307-5337
16. Dobson J.W., Cashion J.P.: Glycol solution drilling system, U.S. Patent No. 6103671 A, 2000
17. EN ISO 12947-1:1998. Textiles - Determination of the abrasion resistance of fabrics by the Martindale method - Part 1: Martindale abrasion testing apparatus
18. EN ISO 5470-2:2003. Rubber - or plastics - coated fabrics - Determination of abrasion resistance - Part 2: Martindale abrader
19. JIS B 0601 – 2001. Surface roughness, Japanese Industrial Standard
20. Singhal A.: The Pearson Guide to Inorganic Chemistry for the IIT JEE 2012. Chapter 1.19. Pearson Education, India, 2011

STUDY OF STICKINESS EFFECT ON FUNGAL DETERIORATION OF COTTON FIBERS

Ivan Lusinyan[1], Elena Pekhtasheva[2], Elena Mastalygina[2] and Kirill Sergeev[1]

[1]Science and Production Innovation Centre of Textile and Light Industry (SPIC TLI), 119071 Moscow, Russia
[2]Academic Department of Commodity Science and Commodity Examination, Academic Department of Chemistry and Physics, Plekhanov Russian University of Economics, 117997 Moscow, Russia
pekhtashevael@mail.ru, elena.mastalygina@gmail.com

Abstract: *In the present study, the influence pattern of cotton fiber stickiness on fungal contamination was studied. By means of DNA analyzing for microscopic fungi (Sanger method), the main biodestructors were identified. Thanks to empirical observation on the behavior of contaminated zones using thermo-detection and analysis of microfungi morphology, visible contamination of cotton with microfungi was defined as an alternative indicator of fiber stickiness determination. Based on the results of this study, a novel method facilitating infected cotton classification was developed.*

Keywords: *cotton fibre, stickiness, biodeterioration, fungal contamination, micromycetes, thermodetection, cotton classing, trehalulose.*

1 INTRODUCTION

Natural, artificial and man-made fibers are common used as raw materials for production of a wide range of fabrics and clothing. Global cotton production and consumption is rising annually. The cotton fiber market attracts manufacturers with the ability to create textiles with high hygienic properties, which more often are in great demand with consumers. Uncontaminated cotton fibers could be produced in the traditional way, but such cotton is characterized by high cost. Manufacturers often use low-quality polluted cotton. Growing in the fields, cotton is exposed to external environmental conditions including atmospheric precipitations, insects, and microorganisms. All these factors cause pollution of cotton fibers, which, in turns, has negative influence on yield value, spinning process and quality of cotton fibers.

The most widespread reason of bacterial and fungal infection of cotton is stickiness (the presence of disaccharides and polysaccharides). The stickiness defect is caused by complex factors as insects securing adhesive sweet liquid that pollutes fibers and microorganisms deterioration [1]. By means of high-performance liquid chromatography of aqueous extracts from cotton, nine main sugars have been found and only one of them is able to block spinning equipment and interfere production. It was a trehalulose ($C_{12}H_{22}O_{11}$) - oligosaccharide, sucrose isomer [2]. A key factor that leads to cotton stickiness due to trehalulose has a low melting point, two or three times lower than for the rest of sugars, according to Heket [3] about 48°C.

Trehalulose is originally entomological sugar and injects on fibers exclusively with secretions (“honeydew”) such cotton pests as aphids (Aphis Gossypii) and whiteflies (Bemisia spp.) [4]. The secret of these insects also contains trehalose, but this saccharide has other chemical and physical properties (melting point, functional groups, etc.).

Honeydew on the surface of cotton fiber could be transferred to a metallic surface of the spinning machines or rubber rollers, etc., resulting in lapping. As a result, it may lower the efficiency of the yarn production and yarn quality [5].

This research investigates interrelation of microscopic fungi deterioration of cotton with its stickiness. The main objective was to study the phenomenon of cotton fiber stickiness and determine whether fungal deterioration is responsible for sticky properties or fungal contamination serves as a consequent effect of stickiness.

2 EXPERIMENTAL

2.1 Materials

The objects of this study were two samples of Central Asian cotton fiber, with different selection and grown in different places. The first sample of cotton fiber is referred to the S-4727 selection supplied by the ginning factory №253 (Myrzakent, Kazakhstan). The second one is the AN36 selection supplied by the ginning factory №069 (Akhunbabaev, Uzbekistan). In this work, a multistage sampling was used according to GOST R 53236-2008 [6]. The cotton samples were exposed in conditions of a temperature of 20±2.0°C and a relative humidity of 65±4%.

2.2 Methods

Cotton Classing

The classing method was used for visual assessment of cotton fiber according to GOST R 53234-2008 [7]. This method was used to determine visible microbial contamination, color, class of weediness and type along the length of the staple formed manually. The special ICS-Texicon equipment was used for providing the lighting in UV range.

High Volume Instrument Analysis (HVI)

HVI analysis was used for testing of length, uniformity in length, strength, elongation at break, micronaire (tinting and maturity), and color. The analysis was performed by USTER HVI 900 SA (CIRAD, France) according to ASTM D5867 [8].

Thermodetection

Thermodetection of cotton fiber samples was carried out by means of SCT thermodetector (CIRAD, France) in accordance with BS EN 14278-1 [9]. The temperature was 84±4°C with hot pressure time of 12±2 s. The force applied was 780±50 N for aluminum hot plate and 590±50 N for an upper wooden board.

Benedict test

To determine the stickiness of cotton fiber Benedict test was performed according to GOST R 53030-2008 [10] (alkaline solution). The numerical values of aqueous extract from cotton fiber was obtained by measuring of optical density (590 nm) using a spectrophotometer PE-5300V (Russia).

Detection of sugar by color reaction

The method of stickiness detection by color reaction was carried out according to ISO 12027:2012 [11]. The droplets of honey dew on a cotton were transferred to paper for color reaction by reagent based on paraaminobenzoic acid. The resulting image on the color reaction paper was compared with a series of standard replicas and the grade was assigned.

DNA sequencing analysis for microscopic fungi (Sanger method)

The specific belonging of microscopic fungi under study is determined by Sanger sequencing analysis carried out by HITACHI Biosystems 3130 (All-Russian Research Institute of Agricultural Biotechnologies, RAAS). The purification of amplicon was performed by Omnix columns. The sequences having length of more than 530 peaks were obtained by using capillary electrophoresis. The obtained DNA sequences were compared with NCBI GenBank international basis [12].

3 RESULTS AND DISCUSSION

According to physical-mechanical analysis by HVI test, the samples under investigation have close parameters of quality (Table 1).

Table 1 Characteristics of cotton fibres under investigation

Parameter		Selection	
		S-4727	*AN36*
Type	Classing	5	6
Code		35	33
Grade		II	II
Class		first	first
Length (UMML) [mm]	HVI test	28.0	25.9
Micronaire		4.2	4.3
Strength [g/tex]		25.5	29.1
Elongation [%]		6.0	6.1
Reflectance [%]		74.1	70.8
Yellowness [+b]		9.9	11.3

The micronaire value is 4.2-4.3, which indicates average roughness of the fibers. The S-4727 selection is characterized by long fibers with average strength (25.5 g/tex), AN36 sample has short fiber length with higher values of strength (29.1 g/tex).

Parameters of color grade defined by HVI meet the results of cotton classing. The cotton samples are medium-fibrous with low trash count. Both the cotton samples have color characteristics from matte-white to cream with pale yellow spots.

However, both samples of cotton are characterized by a high microbial deterioration inspected without magnification. During the classing, numerous black-brown spots being similar to mold fungi contamination were observed on the fiber surface. Figure 1 shows a cotton ball locally affected by microfungi, which was detected by classing.

The thermodetection represents the method for the stickiness determination by simulating the interaction of the working surfaces with fibers, recreating loads and temperatures.

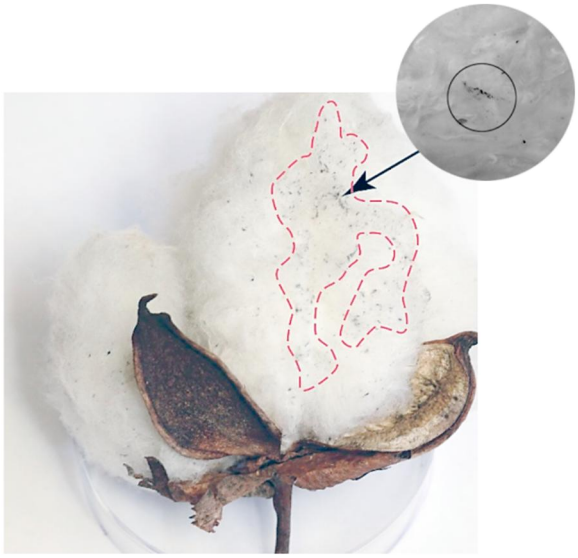

Figure 1 Visible contamination by microscopic fungi easily detectable in cotton fibers at classing (AN36 sample)

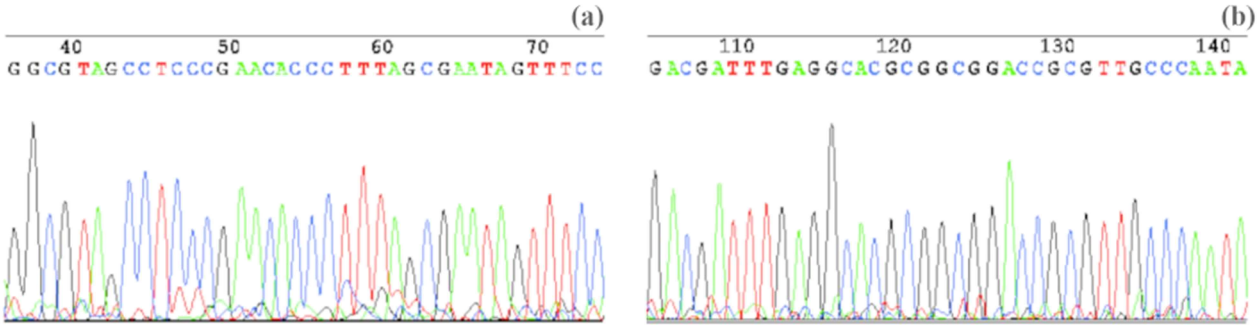

Figure 2 Sequences fragments of the DNA molecules sequencing peaks for the first sample (S-4727 selection)

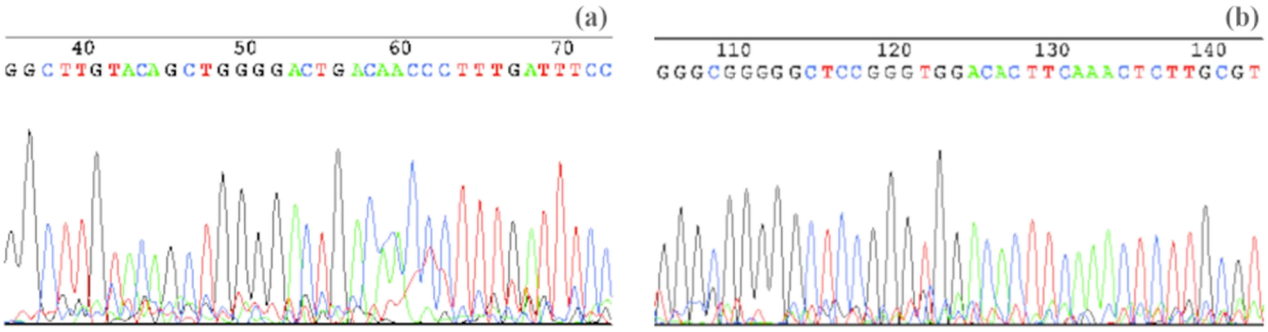

Figure 3 Sequences fragments of the DNA molecules sequencing peaks for the first sample (AN36 selection)

When analysing the stickiness of the cotton samples by the method of thermodetection, the matching of infected zones with the sticky points was fixed. Provided, that exactly these areas were identified as zones of visible contamination by bacterial and fungal infection. In the following, it was necessary to determine the reasons for the concordance of zones affected by microfungi with zones of increased stickiness, and thus to understand whether the fungi are sticky on its own or positioning on the sticky areas defines their presence.

The Sanger analysis results are shown in Figure 2 (S-4727 selection) and Figure 3 (AN36 selection). According to NCBI GenBank database, the fragments sequence of peaks of the both first and second samples are determined as DNA of microfungi *Cladosporium cladosporioides*. Despite the many differences between selected cotton fibre samples (morphology, period of aging, areas of growth), the results of the DNA sequencing method indicate the identity of species of microfungi on both cotton samples.

According to Dugan et al. [13] *Cladosporium* genus includes more than 772 species fouling a variety of crops, including cotton fibers. However, there is no evidence of the ability of *Cladosporium cladosporioides* to release any sticky substances. In case of morphology analysis of *Cladosporium* microfungi, it was stated that the fungal cell wall mainly consists of hexoses (34-47%) and β-1,3-glucan, including a certain amount of galactose and mannose [14]. Galactose and mannose are monosaccharides (hexoses) with a melting point of 167°C and 132°C, respectively. Therefore, such saccharides could not have a significant contribution to stickiness.

Due to the facts that *Cladosporium* does not display the stickiness or release adhesives, the reason of sticky points and visible contamination matching is that fungi use trehalulose as a nutrition source. According to observations of entomologists Rekacha and Dobretsova [15], saprophytic fungi could develop on the cotton aphid excrements, causing further devaluing the fiber quality. As previously noted, the cotton aphid (Aphis Gossypii) and whitefly (Bemisia spp.) emit the “honey dew” containing trehalulose. Consequently, localization of visible fungal contamination could be used for identification of sticky areas and evaluation of infection without using instrumental methods.

Thanks to obtained regularities and the current US classification codes of United State Department of Agriculture (USDA), the system of stickiness rate for infected cotton was developed. The samples of Central Asian cotton fiber (about thirty thousand tons) were assessed by infection intensity. The most typical forms of fungal contamination on fiber revealed were assigned by codes. The photos of typical fungal contamination forms are shown in Figure 4.

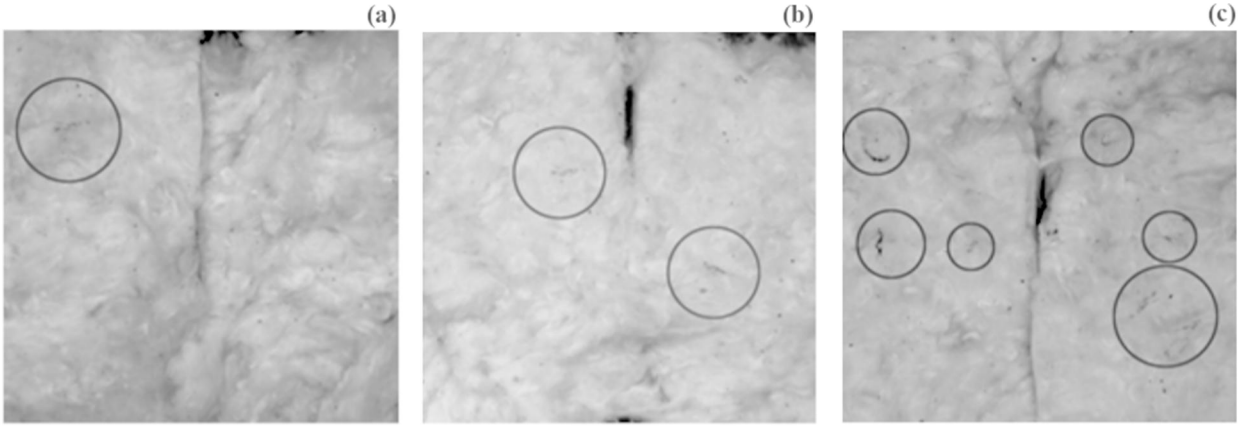

Figure 4 The signs of visible fungal contamination in cotton fibers: low degree – classer code 040 (a), average degree – classer code 041 (b), strong degree – classer code 042 (c)

The developed technique requires using of the visual organoleptic assessment regulations according to GOST R 53234-2008. When cotton sample has separate zones of fungal contamination at least in one of the scanned layers (Figure 4a), it is assigned a code 040. When fungal contamination is observed in two layers of, but not more than two, a cotton fiber sample is assigned a code 041 (Figure 4b), more than two layers - the code 042 (Figure 4c). A code 042 corresponds to strong biofouling that can cause difficulties in processing and be a threat to staff working health (fungal infection). The characteristics of signs according to developed technique of cotton fiber are shown in Table 2. The authors propose to integrate this method of cotton evaluation in GOST R 53224-2008 [16] as an alternative way to identify infected cotton.

Table 2 The assessment system of visible fungal contamination (VFC) degree of cotton fibers

Codes	Brief description	The VFC description
0	None	No signs of VFC
1	Signs of VFC	Barely visible hyphae of microfungi in a separate layer of cotton fiber samples
2	Medium VFC	Noticeable hyphae of microfungi in no more than two layers of cotton fiber samples
3	Strong VFC	Areas of VFC in more than two layers of cotton fiber samples

Classification codes of fungal contamination were convert into numerical values respectively: no code = 0; 040 = 1; 041 = 2; 042 = 3. The results of stickiness index assessing are presented in Table 3.

To compare the accuracy and comparability of stickiness index assessing of cotton fiber using the developed express method and standard techniques, the correlation analysis according to Spearman was performed [17]. Comparative analysis of Spearman rank correlation and statistical reliability of the developed method in comparison with the most-used ones is shown in Table 4.

The data obtained by the developed express method with a high degree of statistical reliability coincide with the data of the advanced thermodetection method, with a correlation of 0.7.

Table 3 Results of the evaluation of cotton fiber stickiness

Method of evaluation		S-4727	AN36
Developed method	code	040 (1)	042 (3)
Thermo-detection (sticky points)	AV	11 (ligth)	37 (strong)
	SD	0.7	0.9
	CV [%]	146.1	14.9
Color reaction (grading)	AV	grade C (medium)	grade C+ (medium+)
	SD	2.3	0.8
	CV [%]	31.2	8.1
Benedict test (solution optical density)	AV	1.05 (strong+)	0.9 (strong+)
	SD	0.4	0.1
	CV [%]	38.1	10.9

Note: *AV* – average value, *SD* – standard deviation, *CV* – coefficient of variation.

Significant differences in results of the developed method and the data obtained by color reaction and Benedict methods are due to the fact that these methods are aimed to determine the total amount of sugars of cotton fiber. However, the total amount of sugars considerably exceeds sugars of entomological origin providing stickiness.

Thus, the developed express method in high degree of reliability characterizes the stickiness of a cotton fiber infected with visible fungal contamination. The developed express method is an alternative, non-labor-intensive way of detecting contaminated cotton when assessing its quality.

Table 4 Comparative analysis of the developed method with the most-used ones

Compared methods	ρ	λ	S' [%]
Developed / thermodetection	0.7	3.2	0.99
Developed / color reaction	0.2	0.7	0.48
Developed / Benedict test	0.2	0.9	0.67

Note: ρ – Spearman rank correlation coefficient, λ – multiplier for statistical reliability, S' – statistical reliability.

4 CONCLUSIONS

The work results prove that microfungi *Cladosporium cladosporioides* found in cotton fibers and identified by DNA sequencing by Sanger are not sticky. The matching of visible microfungi contamination areas with sticky points at thermodetection allows the use of microfungi as an indication of stickiness at the visual cotton classing assessment. The obtained data on cotton classing induces the opportunity to determine the most common forms of fungal contamination and assign. The data obtained according to the developed express method coincides with the data of the most advanced thermodetection method with a high degree of statistical reliability (more than from 99%), with a correlation of 0.7. The proposed methodology allows evaluating the degree of stickiness only for infected cotton.

5 REFERENCES

1. Hequet E., Henneberry T.J., Nichols R.L.: Sticky Cotton: Causes, Effects, and Prevention, United States Department of Agriculture, Agricultural Research Service, 2007
2. Stewart McD.J., Oosterhuis M.D., Heitholt J.J., Mauney R.J.: Physiology of cotton, New York: Springer, 2010
3. Hequet E., Abidi. N.: Processing Sticky Cotton: Implication of trehalulose in residue build-up, Journal of Cotton Science 6, 2002, pp. 77-90
4. Hendrix D.L., Steele T.L., Perkins H.H.: Bemisia honeydew and sticky cotton. Bemisia: Taxonomy, biology, damage, control and management, Andover, UK: D. Gerling and R.T. Mayer, 1995
5. Basra A.S., Saha S.: Growth regulation of cotton fibers / Cotton Fibers: Developmental Biology, Quality Improvement, and Textile Processing, New York: Food Products Press, 1999
6. GOST R 53236-2008. Cotton fibre. Methods of sampling (in Russian)
7. GOST R 53234-2008. Cotton fibre. Methods of color and outward appearance determination (in Russian)
8. ASTM D5867–05. Standard Test Methods for Measurement of Physical Properties of Raw Cotton by Cotton Classification Instruments
9. BS EN 14278-1:2004. Textiles. Determination of cotton fibre stickiness. Method using a manual theromodetection device
10. GOST R 53030-2008. Cotton fibre. Methods for determination of mould contamination (in Russian)
11. ISO 12027:2012. Textiles - Cotton-fibre stickiness - Detection of sugar by colour reaction
12. National Center for Biotechnology Information [official site]. URL: http://www.ncbi.nlm.nih.gov/
13. Bensch K., Groenewald J.Z., Dijksterhuis J., et al.: Species and ecological diversity within the *Cladosporium cladosporioides* complex (Davidiellaceae, Capnodiales), Stud. Mycol 67, 2010, pp. 1-94
14. San-Blas G., Guanipa O., Moreno B., et al.: *Cladosporium carrionii* and *Hormoconis resinae* (C. resinae): cell wall and melanin studies, Current Microbiology 32(1), 1996, pp. 11-16
15. Rekach V.N., Dobretsova T.A.: Cotton aphids in Transcaucasia, Materials on biology and to control them, Tiflis, 1933
16. GOST R 53224-2008. Cotton fibre. Technical conditions (in Russian)
17. Dodge Ya.: The Concise Encyclopedia of Statistics, New York: Springer-Verlag, 2010

ANALYSIS OF A FABRIC DRAPE PROFILE

Tatjana Šarac, Jovan Stepanović and Nenad Ćirković

Faculty of Technology, Leskovac, Bulevar oslobodjenja 124, Universiity of Niš, Serbia,
tangerine.art83@gmail.com

Abstract: *Draping is an important factor in presenting the aesthetics and functionality of textile materials and products. Drape coefficient was used as a numerical indicator of drapery of textile materials. Most authors considered drape coefficient as insufficient parameter for describing the complexity of the concept of drapery, because the two fabrics can have the same drape coefficient and completely different configuration of a drape profile, due to different structural and mechanical properties. The use of software allows measuring many parameters. With the help of these parameters we can explain the drape profile. One of these parameters is circularity, or CIRC, which is a measure of drape profile roundness. This paper investigates the connection between the drape coefficient and circularity in different profiles configuration depending on the structural characteristics of fabrics. The aim of this paper was to study the parameters of drapery that give a better description of the drape profile.*

Keywords: *draping, drape coefficient, circularity, density, structural characteristics, fabric.*

1 INTRODUCTION

The ability of material to drape is a property that undoubtedly defines the qualitative characteristics of the fabric and design of clothing products. Contemporary fashion trends and modern technologies impose increasingly requires to the textile industry. New and functional textile materials, modern methods of making clothes, competition in the world of fashion and clothing are the factors that impose fashion and clothing industry to make constant changes and to adjust to the market requirements.

Draping is an important factor in presenting the aesthetics and functionality of textile materials and products. Generally, draping can be described as a phenomenon of the formation of folds when the fabric is loaded with its own weight without the influence of external forces. Drape coefficient was used as a numerical indicator of textile materials drapery. Drape coefficient describes any deformation between the deformed and not deformed part of the fabric. It is calculated in a percentage as a measure of projected surface of draped fabric and surface uninformed part before draping [1, 2]:

$$DC = \frac{Sp - \pi r_1^2}{\pi r_2^2 - \pi r_1^2} \quad (1)$$

where: *DC* - drape coefficient

S_p – projected surface of draped fabrics, including part covered by horizontal disc, mm^2

r_1 – the radius of the horizontal disc, mm

r_2 –, the radius of the sample before drape, mm

Drape coefficient is often quoted in the literature as insufficient parameter to describe the complexity of the concept of drape. Thus, for example, two fabrics can have the same drape coefficient and completely different profiles or configuration of drape, different structural and mechanical properties. In addition drape coefficient, to describe the drape concept is often used: the minimum and maximum amplitudes, which represent the minimum or maximum distance from the center of the circle to the outline of the profile of the draped sample, and the number of folds [3, 4].

In recent years, various computer softwares were applied for digital determination of the drape coefficient [5]. The photo of a drape profile is captured with a digital camera, and then the captured image is automatically processed to obtain the final image which is adjusted for subsequent analyzes. Using a variety of software enables measurement of many parameters which can explain drape profile. One of these parameters is the drape profile circularity, or *CIRC*. It is a measure of the roundness of a drape profile, as a drape profile shape is closer to form a perfect circle its value is closer to 1 and vice versa [6, 14, 15]. CIRC can be calculated as follows:

$$CIRC = 4\pi \cdot \frac{A}{P^2} \quad (2)$$

where: *A* - surface area of a profile of draped part of sample, *P* - perimeter of the area of draped part of the sample.

2 EXPERIMENTAL

2.1 Materials

For the purpose of draping tests were used different types of raw cotton type fabrics for different end uses (for shirts, dresses, blouses, suits, trousers, work clothes, uniforms). Table 1 shows raw fabrics formed on the same basis in plain weave which differ in density of weft threads. Table 2 shows raw fabrics formed on the same basis in five-wire satin weave but with different linear density of weft threads. Tables 3 and 4 show raw fabrics with different weave and raw material composition.

Table 1 Characteristics of cotton fabrics in plain weave with different weft thread densities

	Sample code	Linear density [tex]		Thread density [cm^{-1}]		Unit weight [g/m^2]	Crimp coefficient		Fabric thickness *h* [mm]
		warp $T_{t,wa}$	weft $T_{t,we}$	warp d_{wa}	weft d_{we}		warp K_{uwa}	weft K_{uwe}	
1	I1	18.52	23.5	37	18.5	127.32	1.184	1.0634	0.45
2	I2	18.52	23.5	36.5	20.5	124.57	1.1742	1.042	0.4
3	I3	18.52	23.5	36.5	21	130.74	1.1544	1.068	0.43
4	I4	18.52	23.5	36.5	23	135.62	1.0574	1.1881	0.41
5	I5	18.52	23.5	37	28	159.01	1.206	1.162	0.39
6	I6	18.52	23.5	37	29	160.57	1,1821	1.164	0.37
7	I7	18.52	23.5	37.5	32	162.65	1.192	1.0633	0.38

Table 2 Characteristics of cotton type fabric in five-thread satin weave with different weft linear densities

	Sample code	Fiber composition [%]		Linear density [tex]		Thread density [cm^{-1}]		Unit weight [g/m^2]	Crimp coefficient		Fabric thickness *h* [mm]
		warp	weft	warp $T_{t,wa}$	weft $T_{t,we}$	warp d_{wa}	weft d_{we}		warp K_{uwa}	weft K_{uwe}	
1	II1	100 Co	100 Co	13.54x2	19.55	43	36	185.65	1.1172	1.0931	0.54
2	II2	100 Co	50/50 Pes/Co	13.54x2	25.04x2	42	32	303.95	1.206	1.0415	0.65
3	II3	100 Co	100 Co	13.54x2	11.13x2	43	31	204.36	1.1164	1.0776	0.53
4	II4	100 Co	33/67 Pes/Co	13.54x2	14.62x2	41	33	228.56	1.1575	1.0368	0.55
5	II5	100 Co	67/33 Pes/Co	13.54x2	14.34x2	41	34	231.21	1.1742	1.03	0.56
6	II6	100 Co	100 Co	13.54x2	24.37	44	35	226.23	1.1152	1.0945	0.56
7	II7	100 Co	33/67 Pes/Co	13.54x2	35.85	43	34	266.14	1.176	1.06	0.59
8	II8	100 Co	50/50 Pes/Co	13.54x2	29.86	42	31	229.36	1.1604	1.052	0.55
9	II9	100 Co	67/33 Pes/Co	13.54x2	20.75x2	43	33	280.76	1.188	1.04	0.61
10	II10	100 Co	67/33 Pes/Co	13.54x2	34.73	40	33	244.6	1.154	1.0435	0.56
11	II11	100 Co	100 Co	13.54x2	17.28x2	46	33	268	1.157	1.086	0.64

Table 3 Characteristics of fabric 50/50% Pes/Co with different weaves

	Sample code	Linear density [tex]		Thread density [cm^{-1}]		Unit weight [g/m^2]	Weave	Crimp coefficient		Fabric thickness *h* [mm]
		warp $T_{t,wa}$	weft $T_{t,we}$	warp d_{wa}	weft d_{we}			warp K_{uwa}	weft K_{uwe}	
1	III1	36.9	28.27	44	27	241.76	panama 3/1	1.1227	1.0328	0.6
2	III2	36.9	28.27	47	26	241.26	warp rib 3/1	1.166	1.0118	0.57
3	III3	36.9	28.27	46	20	221.46	plain	1.115	1.03	0.48
4	III4	36.9	28.27	45	22	231.41	weft rib 3/1	1.1406	1.0699	0.52
5	III5	36.9	28.27	46	22	231.31	weft rib 2/2	1.134	1.0606	0.46
6	III6	36.9	28.27	46	26	245.9	cross twill	1.1450	1.0458	0.53
7	III7	36.9	28.27	45	28	243.65	warp rib 2/2	1.1507	1.0178	0.53
8	III8	36.9	28.27	47	28	243.28	panama 2/2	1.1326	1.036	0.52
9	III9	36.9	28.27	45	27	248.11	twill 2/2	1.1485	1.0421	0.53
10	III10	36.9	28.27	45	26.5	248.93	twill 3/1	1.1535	1.0317	0.5

Table 4 Characteristics of cotton fabrics with different weaves

	Sample code	Linear density [tex]		Thread density [cm^{-1}]		Unit weight [g/m^2]	Weave	Crimp coefficient		Fabric thickness *h* [mm]
		warp $T_{t,wa}$	weft $T_{t,we}$	warp d_{wa}	weft d_{we}			warp K_{uwa}	weft K_{uwe}	
1	IV1	10.84x2	19.98x2	42	32	228.83	twill 4/1	1.2	1.0693	0.61
2	IV2	10.84x2	19.98x2	41.5	31	222.05	twill 3/2	1.1504	1.0673	0.57
3	IV3	10.84x2	19.98x2	42	30	212.72	five-thread satin	1.1343	1.076	0.57
4	IV4	10.84x2	19.98x2	40	33	213.8	mixed panama	1.1816	1.0308	0.64
5	IV5	10.84x2	19.98x2	41	33	210.65	panama 3/2	1.1584	1.0427	0.6
6	IV6	10.84x2	19.98x2	42	31	213.86	panama 3/1	1.1445	1.0096	0.66
7	IV7	10.84x2	19.98x2	39	32	221.97	mixed panams	1.207	1.0217	0.59
8	IV8	10.84x2	19.98x2	43	23	193.38	warp rib 3/2	1.0851	1.124	0.47
9	IV9	10.84x2	19.98x2	44	23	185.52	warp rib 4/1	1.0693	1.099	0.51

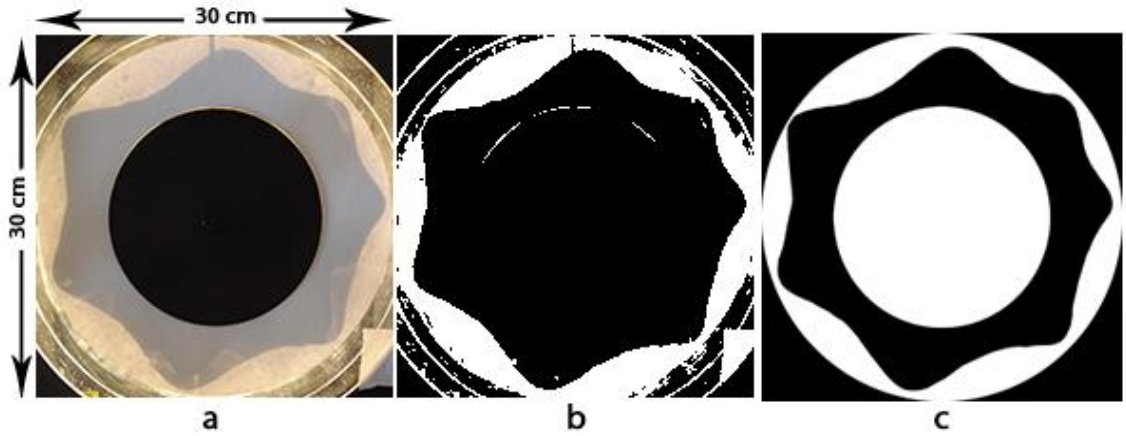

Figure 1 Image processing using Adobe Photoshop: a) cutting and calibration of the image, b) setting the threshold between black and white, c) cleaned image draped sample

2.2 Methods

Determination of drape parameters is carried out on a standardized test device drape tester James H Heal & Co, model 665, according to British standard BS 5058.

For all fabric samples is determined drape coefficient (*DC*), the maximum amplitude (*Amax*) and the minimum amplitude (*Amin*), the number of folds (*n*) and the circularity of a drape profile (*CIRC*).

This experimental method means that circular fabric sample 30 cm in diameter, hangs on a circular disk 18 cm in diameter. The sample with diameter of 36 cm can be used for rigid fabrics if their *DC*% s greater than 85% in fabric sample with a diameter of 30 cm, while in the case of soft fabric can be used 24 cm diameter sample, if their *DC*% in 30 cm diameter fabric sample is less than 30% [6].

However, if would be used a different diameter of fabric samples for this study, the obtained results of drape coefficient could not be in correlation with other parameters of the fabrics, because increasing of draped part of the sample reduces the drape coefficient, so all the fabric samples were tested with a diameter of 30 cm, regardless of the results of drape coefficient which were less than 30% or greater than 80%.

Drape coefficient values were obtained by digital method. By this method, the drape profile of a sample is recorded with digital camera which is mounted on the stand above the drape meter at a certain height so that it covered the top panel of the device, then the resulting image is being processed in software Adobe Photoshop (Figure 1). First is carried out cutting and calibration of the image (Figure 1a), then the image is processed to set the threshold between black and white (Figure 1b). Then it is necessary to clean the image, where on black surface white pixels are removed, and the black pixels on white surface (Figure 1c). Image becomes black - white, and then the surface can be easily marked and number of pixels can be calculated. Adobe Photoshop contains tools for easy and accurate recalculation of pixels in any marked area. The minimum and maximum amplitudes also were measured using pixels measuring the distance from the centre of the circle to the outline of draped profile. All researches were performed under the same conditions.

3 RESULTS AND DISCUSSION

In Tables 5-8 are given the values of the test results of drape coefficient, the minimum and maximum amplitude, the number of folds and drape profile circularity.

Table 5 Test results of cotton fabric drape in plain weave with different weft thread densities

	Sample code	*DC* [%] on the face of the fabric	*DC* [%] on the back of the fabric	*DC* [%]	Minimum amplitude A_{min}	Maximum amplitude A_{max}	Number of folds *n*	Drape profile circularity *CIRC*
1	I1	48.16	47.95	48.06	10.33	14.46	8	0.3035
2	I2	53.21	51.62	52.42	10.74	14.44	7	0.3387
3	I3	51.76	50.88	51.31	10.53	14,47	7	0.3309
4	I4	57.15	57.24	57.19	10.86	14.56	8	0.3733
5	I5	64.7	63.36	63.53	11.44	14.77	7	0.4161
6	I6	68.71	66.46	67.59	11.6	14.71	7	0.4391
7	I7	73.22	70.53	71.87	11.99	14.84	7	0.4578

Table 6 Test results of cotton type fabric drape in five-thread satin weave with different weft linear densities

	Sample code	*DC* [%] on the face of the fabric	*DC* [%] on the back of the fabric	*DC* [%]	Minimum amplitude A_{min}	Maximum amplitude A_{max}	Number of folds *n*	Drape profile circularity *CIRC*
1	II1	44.44	41.56	43	9.34	14.44	7	0.2676
2	II2	76.49	62.91	69.7	11.12	14.84	7	0.4437
3	II3	45.76	42.89	44.33	9.91	14.18	8	0.2783
4	II4	52.81	46.43	49.62	10.14	14.41	7	0.3159
5	II5	57.8	50.58	54.19	10.42	14.69	7	0.3486
6	II6	50.29	46.02	48.15	9.57	14.57	7	0.3466
7	II7	64.56	54.99	59.77	9.9	14.84	6	0.3909
8	II8	62.16	53.47	57.81	10.15	14.77	6	0.3758
9	II9	72.94	62.08	67.51	11.27	14.94	6	0.4341
10	II10	58.34	52.2	55.27	9.57	14.85	6	0.3661
11	II11	57.52	50.03	53.78	10.43	14.53	7	0.3469

Table 7 Test results 50/50 % Pes/Co fabric drape in different weave

	Sample code	*DC* [%] on the face of the fabric	*DC* [%] on the back of the fabric	*DC* [%]	Minimum amplitude A_{min}	Maximum amplitude A_{max}	Number of folds *n*	Drape profile circularity *CIRC*
1	III1	75.55	77.7	76.63	11.15	15.07	5	0.4866
2	III2	75.13	73.83	74.48	11.52	14.94	6	0.4728
3	III3	79	81.7	80.35	11.99	15.02	5	0.5039
4	III4	87.69	89.22	88.45	13.45	15.06	-	0.5861
5	III5	90.1	87.89	89	13.59	15.09	-	0.5419
6	III6	80.73	76.46	78.6	12	15.05	6	0.4927
7	III7	79.16	79.85	79.5	12	15.14	5	0.4984
8	III8	82.63	81.39	82	12.53	15.12	6	0.5072
9	III9	85.77	84.59	85.15	12.75	15.23	-	0.5225
10	III10	82.77	76.85	79.81	12.16	15.06	6	0.4983

Table 8 Test results of cotton fabric drape in different weave

	Sample code	*DC* [%] on the face of the fabric	*DC* [%] on the back of the fabric	*DC* [%]	Minimum amplitude A_{min}	Maximum amplitude A_{max}	Number of folds *n*	Drape profile circularity *CIRC*
1	IV1	62.82	53.34	58.07	10.67	14.7	7	0.3746
2	IV2	65.57	62.53	64.05	11.52	14.64	7	0.4183
3	IV3	66.79	56.7	61.75	10.85	14.65	7	0.4039
4	IV4	63.35	64.5	63.93	11.19	14.67	7	0.4145
5	IV5	59.76	57.62	58.69	10.63	14.58	7	0.3802
6	IV6	62.35	63.73	63.04	11.02	14.75	7	0.4104
7	IV7	65.61	65.71	65.66	11.34	14.73	7	0.4291
8	IV8	57.39	60.72	59.06	11.3	14.47	7	0.3891
9	IV9	64,57	62.49	63.53	11.33	14.6	7	0.4141

Figure 2 shows the relation between drape coefficient and drape profile circularity of cotton fabrics in plain weave (to see changes in drape coefficient depending on changes in weft threads density) and Figure 3 shows the relation between drape coefficient and drape profile circularity of cotton types fabric in satin weave (to be noticed changes in drape coefficient depending on changes in weft linear density). Figures 4 and 5 show the dependence of the drape coefficient and drape profile circularity in fabrics blends 50/50% Pes/Co and 100% cotton fabrics with different weaves applied.

The graphs show that there is a good correlation between drape coefficient and drape profile circularity. The best relation is observed in the fabric where the weft density is changed, r^2 = 0.9919 (Figure 2), and the lowest correlation is with the fabric 50/50 Pes/Co, r^2 = 0.8222 (Figure 4). Determination coefficient in cotton fabrics is (Figure 5) je r^2 = 0.9817, and in cotton types fabrics with changes in weft linear density is r^2 = 0.944 (Figure 3).

According to the graphs, this dependence of drape coefficient and circularity can be represented by regression equation of general form, ie:

$$DC = a + b \cdot CIRC \quad (3)$$

where the coefficients *a* and *b* are given in Table 9.

Circularity as a measure of deviation from a perfect circle is directly related to the appearance draped sample profile. For example, very stiff fabrics that

have no folds and have a slight difference between the value of the minimum and maximum amplitude will have greater value of circularity (closer to 1). Fabrics with a larger number of folds and the greater difference between the values of the minimum and maximum amplitude, will have a lower value of circularity. Figures 6-9 show the appearance of draped sample profiles.

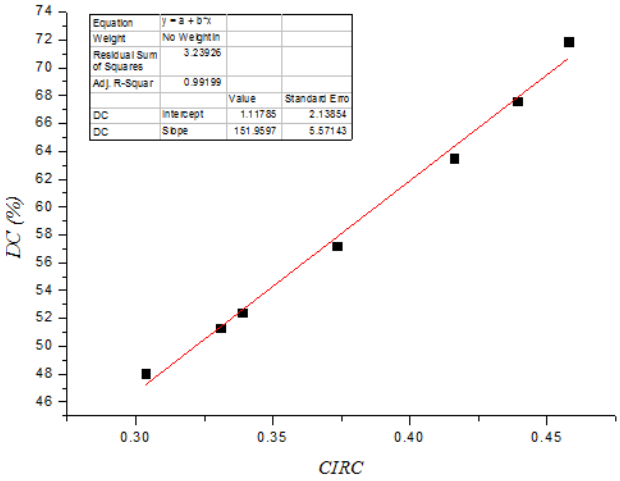

Figure 2 Relation between drape coefficient and drape profile circularity for fabrics with different weft threads density according tables 1 and 5

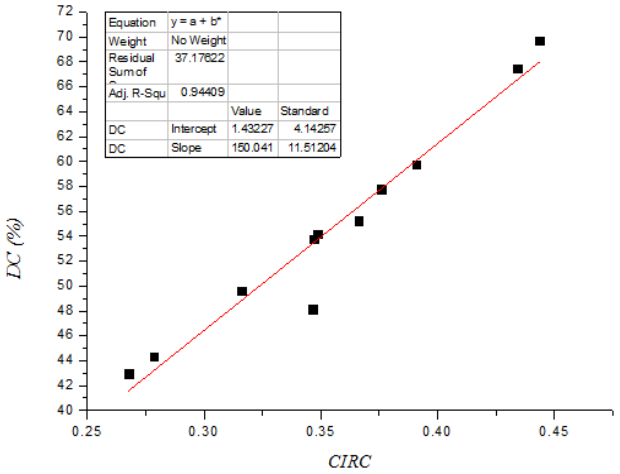

Figure 3 Relation between drape coefficient and drape profile circularity for fabrics with different weft linear density according tables 3 and 6

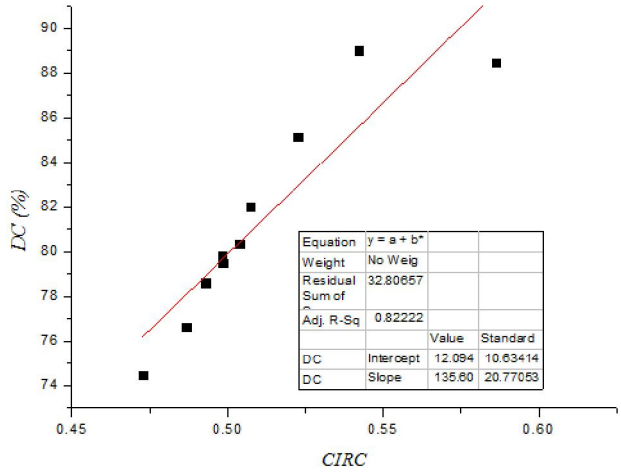

Figure 4 Relation between drape coefficient and drape profile circularity for fabrics 50/50 % Pes/Co with different weaves applied (according tables 3 and 7)

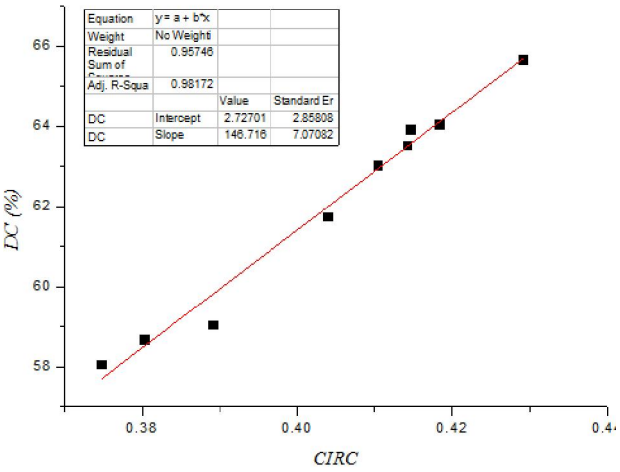

Figure 5 Relation between drape coefficient and drape profile circularity for cotton fabrics with different weaves applied (according tables 4 and 8)

Table 9 The values of the coefficients *a* and *b* of the regression equation $DC = a + b \cdot CIRC$

$DC = a + b \cdot CIRC$	***a***	***b***	r^2
Fabrics with different weft thread densities (Figure 2)	1.11785	151.959	0.9919
Fabrics with different weft linear densities (Figure 3)	1.143227	150.041	0.944
Fabrics 50/50% Pes/Co with different weaves (Figure 4)	12.0948	135.606	0.8222
Cotton fabrics with different weaves (Figure 5)	2.72701	146.7162	0.9817

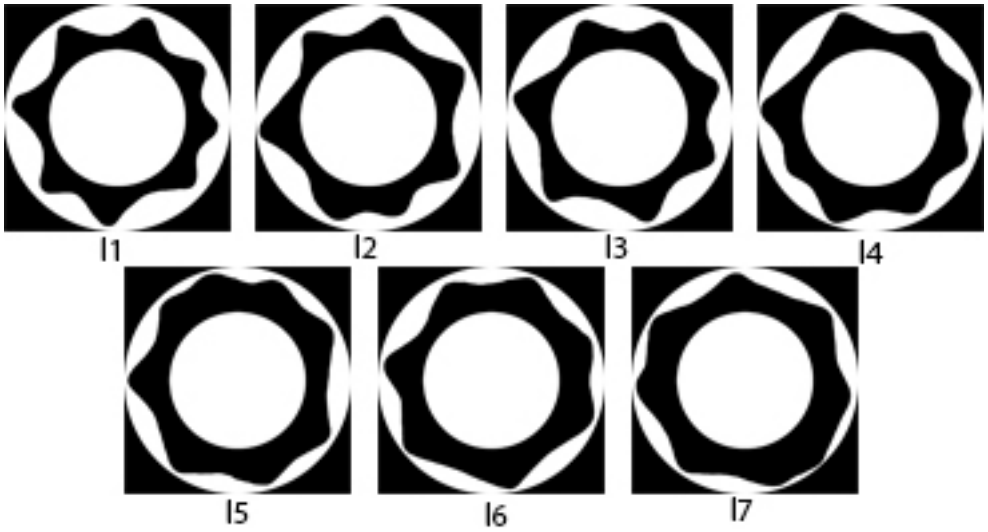

Figure 6 Profile appearance of draped cotton fabric samples from Table 1

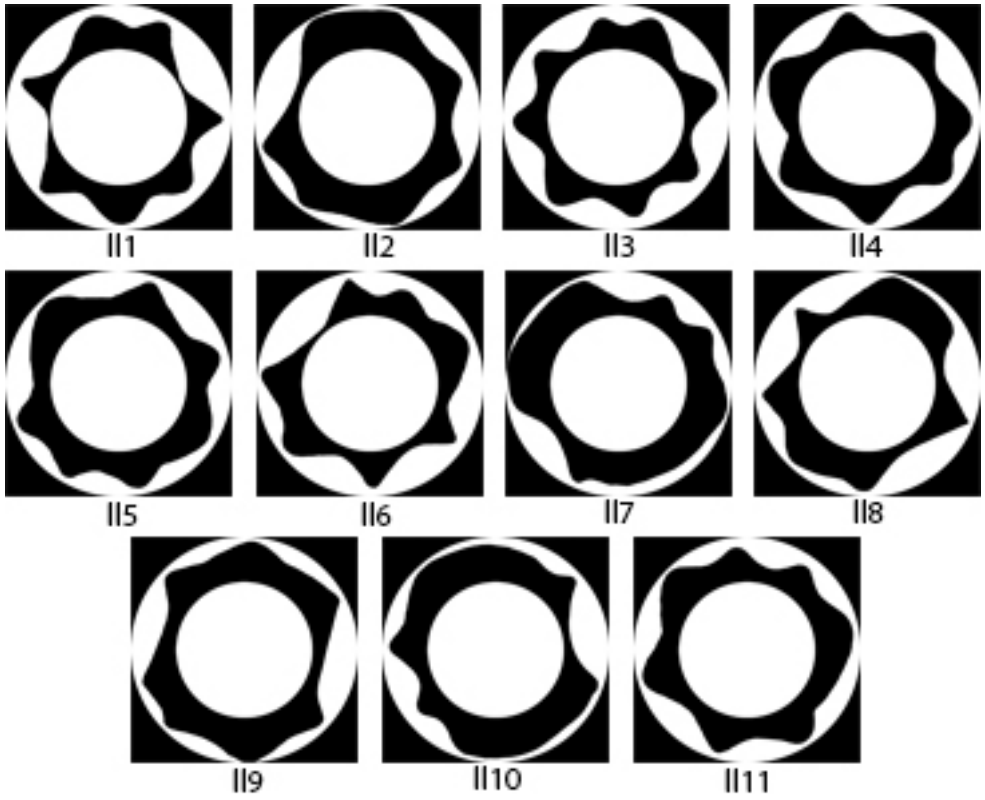

Figure 7 Profile appearance of draped cotton type fabric samples from Table 2

Figure 6 shows profiles of samples of raw cotton fabrics in plain weave with different weft thread density. Based on the results in Table 5 and Figure 6, it can be concluded that with the increase in density of the weft threads, also increase values of drape coefficients (the difference between black and white in the ring), but also increases the value of the circularity. With the higher values of drape coefficient, the differences between values of the minimum and maximum amplitudes are smaller and drape profile tends to perfect circle.

For fabric samples with different linear densities (Figure 7, Table 6), it can be carried out the same conclusion, although from the figure can be seen that these two groups of samples have different appearance of drape profile.

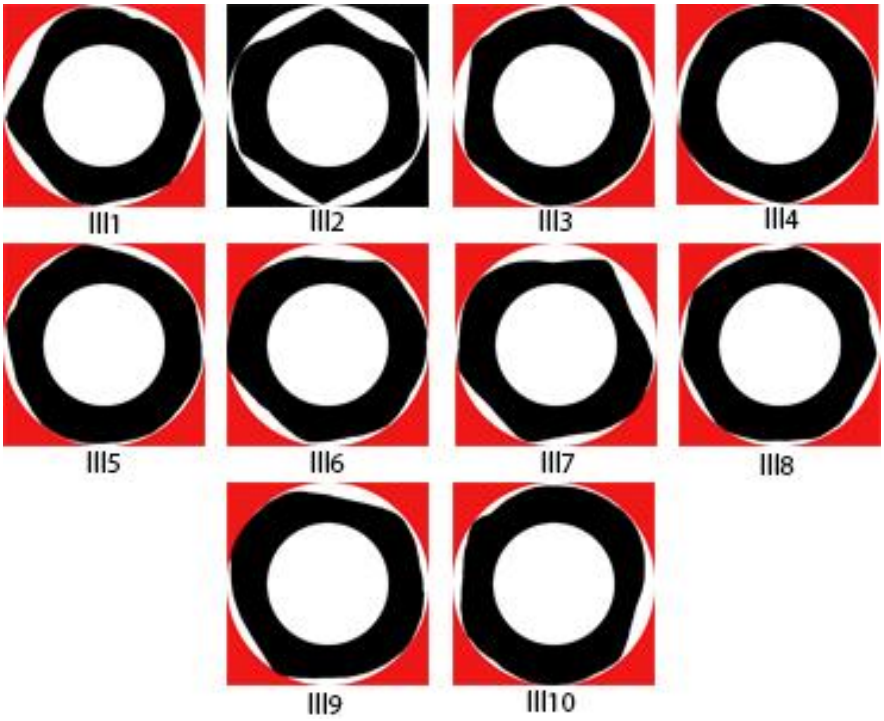

Figure 8 Profile appearance of draped fabric samples 50/50 Pes/Co from Table 3

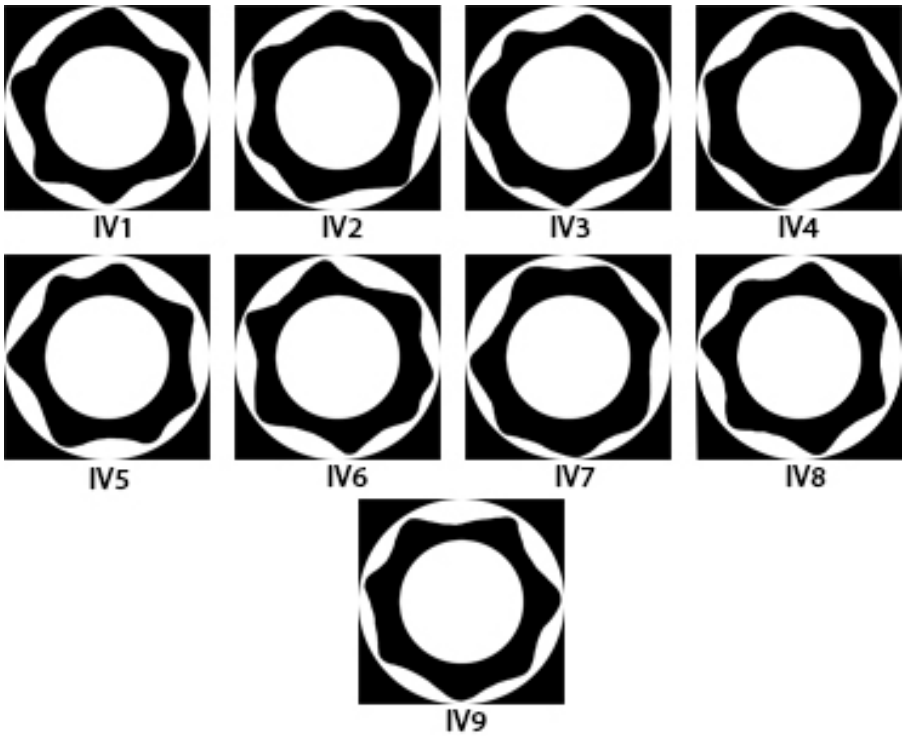

Figure 9 Profile appearance of draped cotton fabric samples from Table 4

On Figures 8 and 9 are shown draped profiles fabric samples in which the changed weave. The samples of fabric from a blend of fibers (50 Pes/50 Co) have significantly higher drape coefficients (Table 7) than samples of cotton fabrics (Table 8), considering that these are a very stiff fabric structures. From Figure 8 and the value of circularity of the drape profile in Table 7, can be seen that samples have a smaller number of folds or no folds and a small difference in values between the minimum and

maximum amplitude. While, on the contrary, with fabric samples in Table 8, drape coefficients have lower values and greater difference between values of the minimum and maximum amplitude, and thus the lower the value of circularity of a drape profile.

4 CONCLUSION

The studies on the draping of textile materials showed that the drape coefficient parameter gives insight into the percentage of the projected part of fabric that folds under the influence of its own weight. However, it is known that the draping of fabric depends on the structural and mechanical properties of the fabric and that these factors affect the configuration of drape profile. Also, two fabrics can have the same values of drape coefficients and completely different configuration drape profiles, which can be interpreted and evaluated as bad or good draping.

For this reason it is necessary to examine other drape parameters that provide detailed insight into the configuration of drape profile depending on the characteristics of the fabric. One such parameter is the drape profile circularity. Therefore, this study examined the connection between the circularity of a drape profile and the drape in different configuration of drape profiles depending on the structural characteristics of the fabric. The results show that the value of drape profile circularity correlated with the values of the drape coefficient, so that using the circularity adds more detailed description of the profile draping of fabric.

5 REFERENCES

1. Lojen D.Ž., Jevšnik S.: Some Aspects of Fabric Drape, Fibres & Textiles in Eastern Europe 15(4), 2007, pp. 39-45
2. Cusick G.E.: A study of Fabric Drape, Faculty of Technology, University of Manchester, 1962
3. Kenkare N., May-Plumlee T.: Evaluation of drape characteristics in fabrics, International Journal of Clothing Science and Technology 17(2), 2005, pp. 109-123
4. HU J.: Structure and mechanics of woven fabrics, Woodhead Publishing Limited in association with The Textile Institute, North America, 2004
5. Kenkare N., May-Plumlee T.: Fabric Drape Measurement: A Modified Method Using Digital Image Processing, Journal of Textile and Apparel, Technology and Management 4(3), 2005, pp. 1-8
6. Robson D., Long C.C.: Drape Analysis using Imaging Techniques, Clothing and Textiles Research Journal 18(1), 2000, pp. 1-8
7. Stylios G.K., Powell N.J., Cheng L.: An investigation into the engineering of the drapability of fabric, Transactions of the Institute of Measurement and Control 24(1), 2002, pp. 33-50
8. Lo W.M., Hu J.L., Li L.K.: Modeling a Fabric Drape Profil, Textile Research Journal 72(5), 2002, pp. 454-463
9. Özdil N., Özgüney A.T., Mengüç G., Sertsöz S.: Influence of yarn and fabric construction parameters on drape and bending behaviour of cotton woven fabrics, Tekstil ve Konfeksiyon 24(2), 2014, pp. 169-179
10. Šarac T., Stepanović J., Demboski G., Petrović V.: Cotton type fabric drape prediction, Industria textila 68(1), 2017, pp. 3-8
11. Šarac T., Stepanović J., Demboski G., Petrović V.: Fabric draping and cotton fabric structure relation analysis, Advanced Technologies 4(1), 2015, pp. 84-88
12. Nofitoska M., Demboski G., Carvalho M.A.F.: Effect of fabric structure variation on garment aesthetic properties, Tekstil ve Konfeksiyon 22(2), 2012, pp. 132-136
13. Saville B.P.: Physical testing of textiles, Woodhead Publishing Limited in association with The Textile Institute, Abington Hall, Abington, 2000
14. Sanad R., Cassidy T., Cheung V., Evans E.: Fabric and Garment Drape Measurement - Part 2, Journal of Fiber Bioengineering and Informatics 6(1), 2013., pp. 1-22
15. Kenkare N.S.: Three dimensional modeling of fabric drape, North Carolina State University, 2005

EFFECT OF ELASTIC ELONGATION ON COMPRESSION PRESSURE AND AIR-PERMEATION OF COMPRESSION SOCKS

Hafiz Faisal Siddique, Adnan Ahmed Mazari, Antonin Havelka, Sajid Hussain and Tariq Mansoor

Department of Clothing Technology, Faculty of Textile Engineering, Technical University of Liberec, Studentská 2, Liberec, Czech Republic
hafiz.faisal.siddique@tul.cz; adnanmazari86@gmail.com; antonin.havelka@tul.cz; sajid.hussain@tul.cz; tariq.mansoor@tul.cz;

Abstract: *The aim of this research is to analyze effect of varying leg sizes on lateral compression pressure at ankle and calf portions and mutual graduation [%]. We also studied the effect of transverse elastic elongation [%] on air permeation [mm/sec] in relaxed (0% extension) and extended state (70% extension) of compression socks. To extend the compression socks at ankle and calf portions, a novel extension frame was used. Kikuhime pressure measuring device was used for measuring lateral compression and mutual graduation [%]. As far the comfortability of compression socks is concern, it was a great challenge to mitigate and convince the patients to use the compression socks who do not prefer to use due to ''too much hotness" and 'itching' registered in various studies. Air permeation tester was used for measurement of air permeability properties at ankle and calf portions of compression socks in relaxed and extended state. In this study, we found that as the elastic elongation in transverse direction of compression socks at ankle and calf portion increases, a significant change in lateral compression and air permeation was observed. We concluded that as the circumference of leg increases, a significant increase in compression pressure takes place. Air-permeation has also been changed with change in elastic elongation significantly (p value<0.05). Out the three socks samples the best sample was rib structured compression socks.*

Keywords: *Compression socks, Kikuhime device, Air-permeation.*

1 INTRODUCTION

Compression socks are the highly acclaimed textile garment for pressure exertion on the lower part of the leg. It is used to reduce venous hyper pressure [1]. Mechanism of action is lowering of pressure exertion from ankle to calf portion of the leg. This varying degree of compression pressure propagate and regulate blood flow, keep the muscles in-line at the right position to mitigate the injury risk, gives relief to many of chronic venous disease patients and used for therapeutic purposes [2, 3].

The intensity of compression pressure used for various diseases is categorized as moderate up to (20-30 mmHg) and firm compression (30-40 mm Hg). This extent of pressure is decided and recommended to treat circulatory and vascular medical conditions as well for tired, sore, swollen, or aching legs [4-7].

Theoretically, the extent of compression socks pressure depends on the leg radius *r* and reversal force *T* [N] around the leg can described by Laplace's Law [8] that is:

$$P = \frac{T}{r} \tag{1}$$

where: *P* - pressure [Pa]; *T* - reversal fabric tension [N]; *r* - radius of leg [cm].

For human leg, circumference is required so equation (1) can be modified to:

$$P = \frac{T \times 2\pi}{C} \tag{2}$$

where: *P* - pressure [Pa]; *T* - reversal fabric tension [N]; *C* - circumference of leg [cm].

For upward blood flow, graduation in socks is of great importance from ankle to calf portion is calculated using formula:

$$G = \frac{P^c}{P^a} \times 100 \tag{3}$$

where: P^c - pressure at calf portion [Pa]; P^a - pressure at ankle portion [Pa].

As per literature review and equation (2), it can be concluded that lateral compression and graduation% (G %) in compression socks depends on its circumference and reduction%.

Reduction percentage% is actually the difference in the circumferential dimension of leg and compression socks at a specific point (ankle/calf). It can be calculated using below formula [7, 9-11]:

$$R = \frac{L - S}{L} \times 100 \tag{4}$$

where: *R* - width reduction [%]; *L* - leg width [cm]; *S* - socks width [cm].

In actual practice, when any pressure garment is worn, it extends to some extent. This stretch generates tension in the yarns which exert radial

pressure on the curved human limb. In [11] is mentioned that practical elongation of compression sock of standard size must be extended to 50% maximum transversely.

This stretch also changes the loop shape, density and thickness of fabric. All these changes are expected to affect the comfort behavior of fabrics especially air permeation, thermal effusivity and thermal conductivity across the compression socks is analyzed and factors affecting the same.

Because of the extreme sensitivity of skin in the affected area, comfort characteristics of compression socks play a critical role in patient's compliance and healing.

Seshadri et al. [12] studied the use, compliance and efficacy of compression socks. In their study they analyzed 3,144 patients for tertiary venous practice. They concluded that only 21% patients uses stockings on daily basis, 12% most days, 4% used less option, 63% don't use. They inquired the reasons: 30% unable to give reason, 25% not recommended by physician, 14% did not help, 14% binding off, 8% too hot to wear, 2% limb soreness, 2% due to itching and 2% others (cost and work station). As far as pressure exertion and graduation in socks plays an important role to control re-occurrence of venous ulcer and venous insufficiency. It should exhibit optimum comfort properties to regulate heat and moisture transfer (comfortness) generated during different physical activities of patients.

Gupta et al. [13] studied the comfort properties of pressure garments at different extension levels from 0 to 60%. They extended the fabric by designing a frame (30×30 cm^2) made up of acrylic sheet and took sample of 14.4 cm×20 cm and marked square of 10×10 cm^2. But for compression socks this frame cannot be recommended as socks circumference at ankle is very low and higher at calf. For Compression class III and IV it is very hard to extend to 60% precisely. Wang et al. [14] mentioned the same while investigating dynamic pressure attenuation of elastic fabric for compression garment.

Fundamental parameters which govern the thermo-physiological properties of fabrics are fibre type, fibre conductivity, fibre moisture regain, yarn count, yarn twist per inch, yarn structure, spinning process, fabric structure, fabric loop length, fabric thickness, fabric porosity and finishing treatments [15].

Air flow through textiles is mainly affected by the pore characteristics of fabrics. It is quite clear that pore dimension and distribution is a function of fabric geometry. The yarn diameter, surface formation techniques and the number of loop, counts per unit area are the main factors affecting the porosity of textiles. The porosity of a fabric is connected with certain of its important features, such as air permeability, water permeability, dyeing properties etc. [15, 16].

Benltoufa et al. [16] investigated methods of determining jersey porosity, which proved that geometrical modeling is the most suitable and easiest method of determining porosity It was determined that porosity depended on fabric parameters and relaxation progression.

Fabric properties related to thermal behavior are bulk density, porosity and air permeability was determined. Total porosity of the knits *P* [%], defined as the portion of all air spaces in knitted fabric both between yarns and inside them, was determined according to the following equation:

$$P = 100 - \frac{\delta}{\rho} \times 100 \quad (5)$$

where: *P* - porosity; *ρ* - fiber density [g/m^3]; *δ* - bulk density [kg/m^3] [17].

$$P = 1 - \frac{m}{\rho . h} \times 100 \quad (6)$$

where: *P* - porosity; *m* - fabric areal density [g/cm^2]; *ρ* - fiber density [g/m^3]; *h* - thickness [cm] [18].

To extend the compression socks at ankle and calf portion, it was very challenging to design a frame that can elongate the socks samples with more precision and accuracy in uni-axial direction. For this, novel extension frame was introduced.

The aim of this study was to investigate the effect of elastic elongation on air permeation [mm/sec] to get rid of sweat accumulation between garment and skin in relaxed and extended state.

It was also studied the effect of 2 different leg sizes on compression pressure

2 MATERIALS AND METHODS

Three type of compression socks were purchased and structurally analyzed with great precision and accuracy.

2.1 Physical testing of compression socks

All the three sock samples were evaluated for courses and wales per inch using pick glass in relaxed (0% extension) and extended state (up to 70% extension). Thickness of fabric was measured using Digital thickness tester of type M034A, SDL (Atlas) according to standard test method along with porosity. Physical testing results of socks samples are given in Table 1.

Table 1 Physical testing of compression socks in relaxed state (0% extension)

Sample codes	Position	BIISJ*	BIIISJ*	DGIIRIB*
Socks circumference [cm]	Ankle	16.6	16	16.4
	Calf	23	25.6	26
Courses/cm	Ankle	144.80	124.50	142.20
	Calf	147.32	124.46	58147.32
Wales/cm	Ankle	132	124.46	106.70
	Calf	106.70	91.5	68.60
Stitch/cm^2	Ankle	1168.40	944.90	924.5
	Calf	705.10	693.42	617.22
Thickness b [mm]	Ankle	0.75	0.95	1.20
	Calf			
Areal density [g/m^2]	Ankle	308.80	378.47	350.97
	Calf	291.80	368.47	292.47
Porosity [%]	Ankle	64.19	65.35	74.56
	Calf	66.16	66.27	76.23

BIISJ BIIISJ- beige-compression level-single jersey; *DGIIRIB- dark grey- compression level-rib structured.

2.2 Characterization of compression socks

Pressure measurement

Three socks samples were worn on human legs of two different circumferences *L1* and *L2*. Due to different circumferences, it exhibit varying reduction percentages *R1* and *R2* [%] calculated using equation (4), mean compression pressure values *P1* and *P2* [mm Hg] using pressure measuring device and mutual graduation percentages *G*; *G1* and *G2* [%] were calculated using equation (3) as mentioned in Table 2.

Pressure was measured by sitting upright on a flat seat chair with flat backrest at 45 cm high from the floor using Kikuhime (TT med, Denmark) pressure measuring device. The probe of pressure measuring device was placed between socks and skin at ankle and calf portions simultaneously as shown in Figures 1 and 2.

Figure 1 Pressure measurement in sitting position (single jersey)

Figure 2 Pressure measurement in sitting position (Rib)

2.3 Novel extension frame

When compression socks worn it extends to both longitudinal and horizontal direction according to circumference and length of leg. Various studies exist in which we found that the socks are extended to maximum 60% depending on extent of pressure (20 to 40 mm Hg) relates to intensity of the disease (Edema to venous Ulcer).

Novel extension frame is drived using combination of three gears as shown in Figure 2. Middle gear, connected with revolving handle, drives the two movable jaws in opposite direction. Maximum distance between jaws can be achieved up to 36 cm. As we rotate the handle, the jaws move apart and extend the fabric to required level (up to 70% and more). Total length of frame is 40 cm; width of jaws is 14.5 cm.

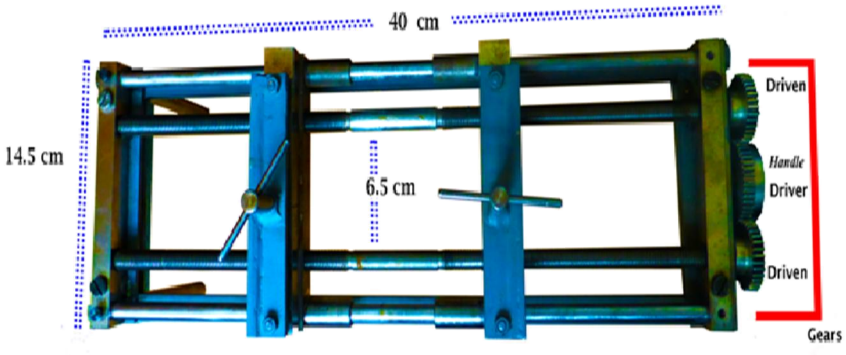

Figure 3 Novel extensibility frame

Table 2 Legs circumferences vs compression pressure

Sample codes	Position/symbols	*BIISJ	*BIIISJ	*DGIIRIB
Socks circumference [cm]	Ankle	16.6	16	16.4
	Calf	23	25.6	26
Socks areal graduation [%]	G	72.17	62.5	63.07
Leg circumference *L1* [cm]	Ankle		22±0.5	
	Calf		35±0.5	
Reduction *R1* [%]	Ankle	24.54	27.27	25.45
	Calf	34.28	26.85	25.71
Pressure *P1* [mm Hg]	Ankle	26±1	37±1	21±1
	Calf	22±1	29±1	14±1
Pressure graduation *G1* [%]	G	84.61	78.37	66.66
Leg circumference *L2* [cm]	Ankle		24.5±0.5	
	Calf		38.5±0.5	
Pressure graduation *G2* [%]	G	85.71	78.37	66.66
Reduction *R2* [%]	Ankle	32.24	34.69	33.06
	Calf	56.88	58.44	57.40
Pressure *P2* [mm Hg]	Ankle	35±1	42±1	25±1
	Calf	30±1	40±1	24±1
Pressure graduation *G2* [%]	G	85.71%	95.23	96%

BIISJ BIIISJ- beige-compression level-single jersey; *DGIIRIB- dark grey- compression level-rib structured.

2.4 Air permeability measurement

All the three socks were cut in longitudinal direction and allow them to be relaxed for long time under standard test method AATCC 99.

Air permeability of all samples in relaxed state and in extended state was measured accordingly to EN ISO 9237:1995 using Air permeability tester. Air pressure of 20 Pa was set across the surface of compression socks. The measuring area of the sample and machine was 20 cm^2. Average of at least 10 values were measured under controlled laboratory conditions of 20±2°C, 65±4% relative humidity and analyzed using Mintab 17 data analysis. Air permeability is measured as:

$$AP = \frac{qv}{A} \times 10 \quad (7)$$

where: $q\nu$ - volumetric air flow per second [cm^3/sec]; *A*- area [cm^2] [19, 20].

Air permeability in relaxed and extended state

All socks samples (8×8 cm), were installed on air permeability machine one by one and notified for air permeability results in relaxed state. Then all samples were re-installed on novel extension frame and calibrated with previously measured values in relaxed state (at 0% extension) at ankle and calf portion simultaneously. Once the same values obtained before and after installation of socks at extension frame, we started notifying values from relaxed state (*L0*, 0% extension). We continued to notify the volumetric air flow (cm^3/sec) after periodical increment of 10% extension up to 70% for each cut samples. For each reading, the distance between the jaws was measured as initial value (*L0*) and then extended maximum up to 70% (*L70*) with increment of 10% increase in distance between the jaws (*L10, L20, L30, L40, L50, L60* and *L70*). Air volumetric flow at each 10% incremental distance was measured as shown in Figure 4.

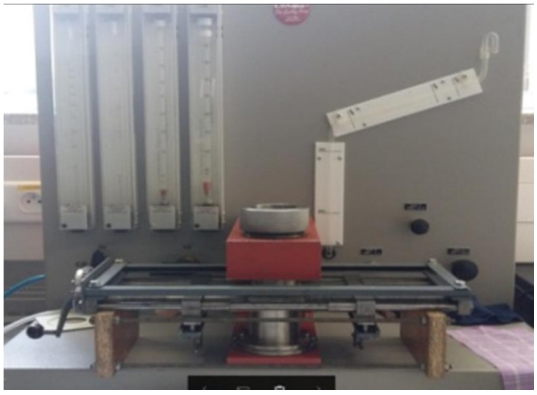

Figure 4 Air permeability measurements (front view)

3 RESULTS AND DISCUSSION

3.1 Compression pressure measurements

Effect of leg circumference on compression pressure at ankle

Table 2 and Graph 1 depict the change in compression pressure; *P1* and *P2* and reduction percentages; *R1* and *R2* among three socks samples (BIISJ, BIIISJ and DGIIRIB). Firstly, we worn BIISJ socks samples on leg *L1* and then on leg *L2*, exhibiting circumferences at ankle *L1* 22±0.5 cm and *L2* 24.5±0.5 cm, we found an incredible increase in compression pressure at ankle from *P1* 26±1 mm Hg to *P2* 35±1 mm Hg along with increase in reduction percentage from *R1* 24.54% to *R2* 32.24%. For socks samples BIIISJ, we also found an incredible increase in compression pressure from *P1* 37±1 to *P2* 42±1 as well as in reduction percentage from *R1* 27.27% to *R2* 34.69% while for socks samples DGIIRIB, compression pressure was increased from *P1* 21±1 to *P2* 25±1 while reduction percentage from *R1* 25.45% to *R2* 33.06%.

Effect of leg dimension on compression pressure at calf

Table 2 and Graph 2 depict the change in compression pressure and reduction percentage between due to change in circumference of leg at calf portion.

When worn BIISJ socks samples on leg *L1* and then leg *L2*, exhibiting circumferences values 35±0.5 and 38.5±0.5 cm simultaneously, we found an incredible increase in compression pressure *P1* 22±1 to *P2* 30±1 mm Hg, as well as reduction percentage from *R1* 34.28 to *R2* 56.88%. For socks sample BIIISJ, we found an incredible increase in compression pressure from *P1* 29±1 to *P2* 40±1 and reduction percentage from *R1* 26.85 to *R2* 58.44%. Similarly, for DGIIRIB, increase in compression pressure from *P1* 14±1 to *P2* 24±1 as well as in reduction percentage from *R1* 25.71 to *R2* 57.40% was observed.

Effect of leg dimension on gradation percentage G [%]

Table 2 and Graphs 3 portray the change in graduation percentage G [%] between the three socks samples (BIISJ, BIII SJ and DGIIRIB) due to change in circumference of two legs *L1* and *L2* at ankle and calf portions of compression socks.

We found that as leg size *L1* changes to *L2* (specifications mentioned in Table 2), there is an incredible change in graduation percentages of all the three socks samples BIISJ, BIII SJ and DGIIRIB occurs from *G1* 84.61, 78.37 and, 66.66% to *G2* 85.71, 95.23 and 96% simultaneously cause reverse flow of blood ultimately happening of hypertension inside the veins and muscles.

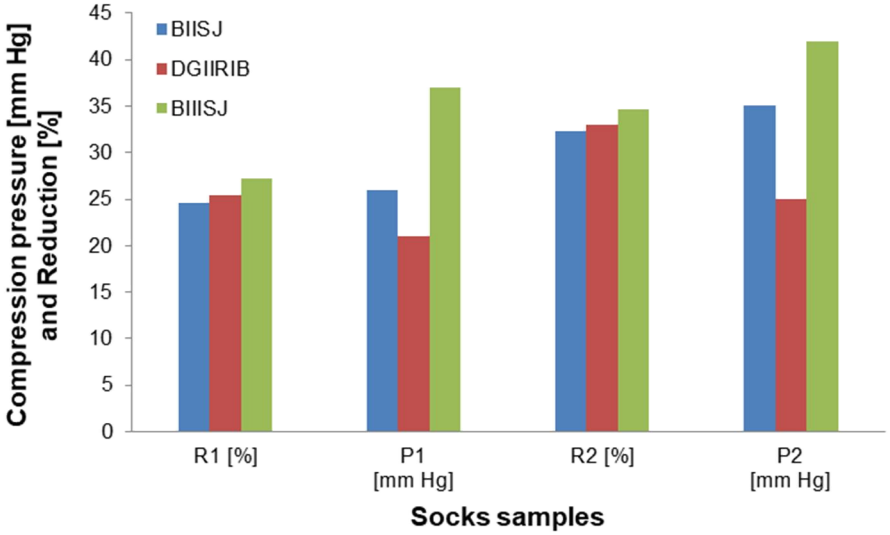

Graph 1 Reduction percentage [%] and compression pressure [mm Hg] at ankle vs leg circumference (*L1* to *L2*)

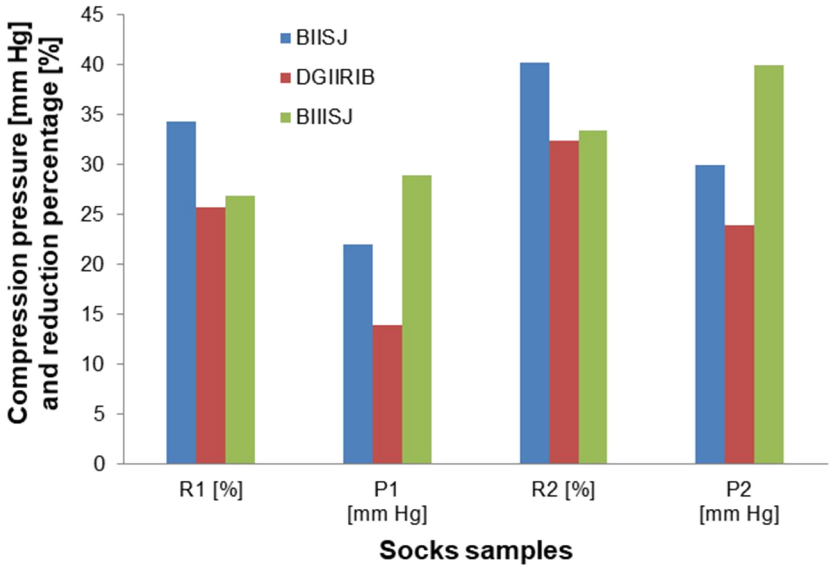

Graph 2 Reduction percentage [%] and compression pressure [mm Hg] at calf vs leg dimension change (*L1* to *L2*)

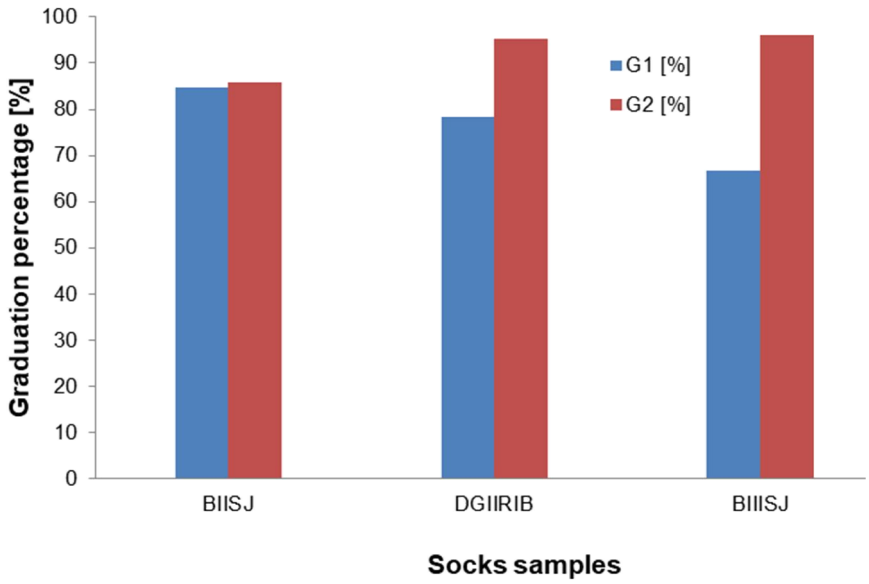

Graph 3 Effect of leg circumference change on graduation percentage G [%]

3.2 Air permeability measurement

Air permeability values of all the socks samples at ankle and calf portions of compression socks were measured at various levels; relaxed state (0% extension) and then to extended state (up to 70% extension). The results are plotted and analyzed using Minitab 17 using regression analysis tool as shown in Graphs 4-5 and Tables 3-4.

Air permeation in relaxed state (0% extension)

Table 1 shows the results of stitch density per inch^2, porosity and air permeation of all the three socks samples in relaxed state (0% extension). Out of three socks samples, BIISJ, BIIISJ and DGIIRIB, we conclude that DGIIRIB sample exhibit the highest value of air permeation 22 mm/sec at ankle then calf portion 25 mm/sec as shown in Graphs 4 and 5. This is due to the lowest value of stitch density i.e. 364 stitches per inch^2 and the highest value of porosity i.e. 74.56 than rest of 2 socks samples BIISJ and BIIISJ at ankle. While socks samples DGIIRIB, exhibit lower stitch density of 343 stitches per inch^2 and higher porosity (76.23) at calf portion than at ankle due which it allows more air 25 mm/sec to flow than at ankle portion of socks samples.

Air permeation in extended state

Table 3 and graphs 4-5 portray effect of elastic elongation on stitch density and its ultimate effect on air permeation at ankle and calf portions as well. Table 4 depicts the regression relation between elastic elongation and air permeation at ankle and calf portion as well.

Air permeability values of all the socks samples at ankle and calf portions of compression socks were measured at various levels; relaxed state (0% extension in Table 2) to extended state (70% extension in Table 3).

The results are plotted and analyzed using Minitab 17 regression analysis tool as shown in Graphs 4–9 and in Tables 2 and 3.

Air permeation [mm/sec] in relaxed state at ankle and calf portion of compression socks

Table 3 shows the results of stitch density per inch^2 and porosity that was measured using equation (5) and equation (6).

We found that out of three compression socks samples BIISJ, BIIISJ and DGIIRIB when evaluated in relaxed state for air permeability, sample socks DGIIRIB acquired the maximum flow of air at ankle portion i.e. 22 mm/sec. but the at calf portion air permeation was 25 mm/sec.

Graph 4 portray that air permeability of socks sample DGIIRIB exhibit highest value of air permeation 22 mm/sec with the lowest value of stitch density i.e. 364 stitches per inch^2 and the highest value of porosity i.e. 76.27% than rest of 2 socks samples BIISJ and BIIISJ at ankle while at calf portion the stitch density and porosity is higher that ankle due to which the air permeation is higher at calf portions of compression socks than at ankle portion i.e. 22 mm/sec but the at calf portion air permeation was 25 mm/sec.

Effect of elastic elongation on air- permeability (at ankle)

Graph 4 and Table 3 depict that when we extend the socks from relaxed to extended state, we found an incredible increase in flow of air across socks sample takes place. It is due to decrease in stitch density [stitches per inch^2].

Out of three samples, BIISJ, BIIISJ and DGIIRIB, we observed DGIIRIB exhibit highest permeation of air flow 22.5 mm/sec than rest of two socks samples BII9SJ, BIIISJ exhibit 4.5 mm/sec and 11.5 mm/sec at relaxed state.

We also observed when it was extended to 70% extension acquiring the values 190 mm/sec while rest of two socks samples, BIISJ and BIIISJ exhibit 75 mm/sec and 150 mm/sec successively. The reason of higher permeation of air across DGIIRIB is due to successive decrease in stitch density per inch^2 as well as increase of pore size of socks samples.

Statistical effects of elastic elongation (0% to 70%) of all samples were evaluated by Minitab 17 using simple regression tool.

The results of regression analysis of effect of elastic elongation on air permeation are analyzed with *p* value<0.005 (at 95% significant level) and other related parameters mentioned in Table 4.

Table 3 Air permeability vs stitch density results in extended state

Position	Socks Code	Parameters	Extension [%]							
			0	10	20	30	40	50	60	70
Ankle	*BIISJ	stitches/cm^2	1168.40	1094.70	1043.90	992.40	936.5	889	861	821.7
Calf			959.10	906.8	850.9	792.50	756.9	708.6	675.6	635
Ankle		AP [mm/sec]	4.5	10	13.5	25	35	50	62.5	75
Calf			5	12.5	18.5	35	45	60	75	110
Ankle	*BIIISJ	stitches/cm^2	944.90	892.80	838.2	784.90	731.5	685.7	640	589.30
Calf			693.4	640	584.2	528.8	492.76	454.66	417.5	381
Ankle		AP [mm/sec]	11	18	30	40	60	87.5	107.5	150
Calf			11.5	22.5	40	52.5	95	120	157.5	200
Ankle	*DGIIRIB	stitches/cm^2	924.56	863.8	800.10	759.56	718.82	655.30	589.3	525.8
Calf			617.20	574	530.86	510.54	464.82	421.64	400	378.46
Ankle		AP [mm/sec]	22.5	29	35	45.25	82.5	110	150	190
Calf			25	27.5	50	72.5	107.5	150	190	220

BIISJ BIIISJ- beige-compression level-single jersey; *DGIIRIB- dark grey- compression level-rib structured.

Table 4 Statistical analysis of each parameter

Socks Code	Parameters	Position	R-Square Value	p value<0.05	Correlation	Regression Equation
BIISJ	Air Permeability	Ankle	94.41	*0.001	0.97	Y= -4.125 + 1.407X
		Calf	97.15	*0.001	0.99	Y= -2.042 + 1.042X
BIIISJ		Ankle	95.55	*0.001	0.97	Y= -7.500 + 2.711X
		Calf	93.83	*0.001	0.97	Y= -4.208 + 1.920 X
DGIIRIB		Ankle	96.43	*0.001	9.8	Y= 0.625 + 2.991 X
		Calf	91.82	*0.001	0.96	Y= -1.96 + 2.428X

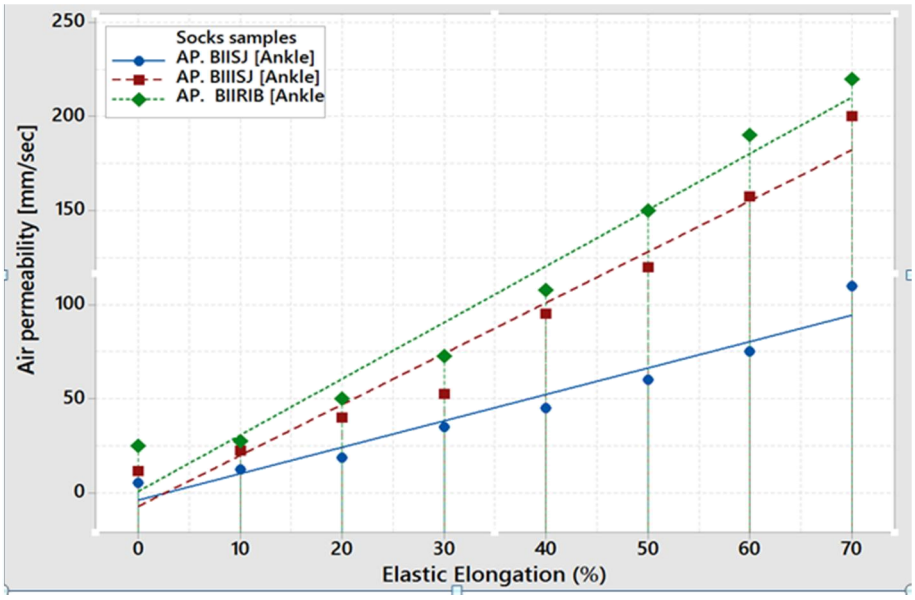

Graph 4 Effect of elastic elongation and stitch density on air permeability at ankle

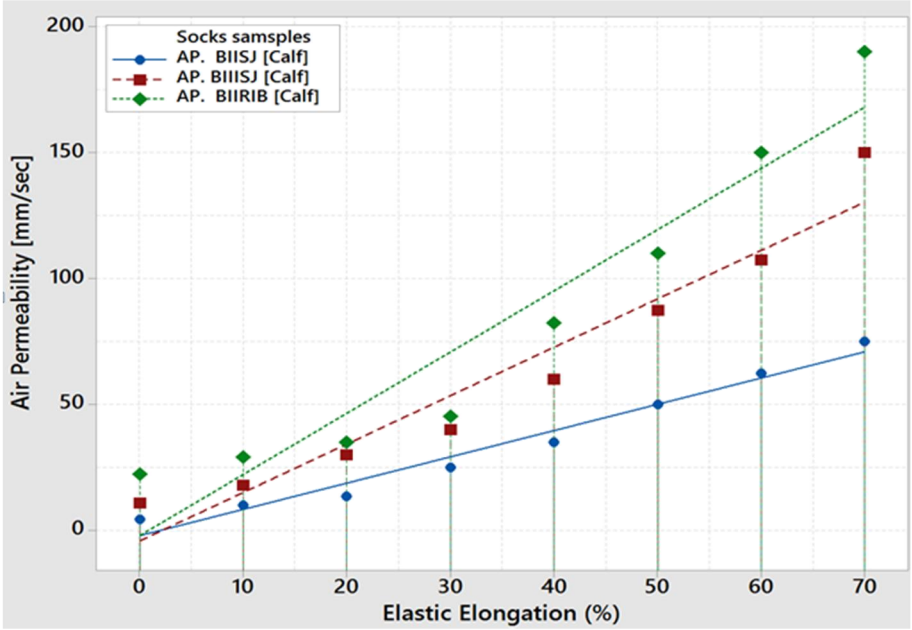

Graph 5 Effect of elastic elongation [%] and stitch density on air permeability at calf

Effect of elastic elongation on air permeability (at calf)

Graph 5 and Table 3 portray that as elastic elongation increases from 0% extension to 70% extension, an incredible increase in air flow across the samples has occurred.

Out of three socks samples, it was found that the socks sample DGIIRIB exhibit the highest permeation of air as it exhibit rib construction and minimum stitches density and higher distribution of pores per unit area as shown in Graph 4 and testing results mentioned in Table 3.

Statistically effect of elastic elongation (0 to 70%) of all the socks samples were evaluated by Minitab 17 using simple regression tool. We found that elastic elongation significantly affect, p value <0.005, quantitative flow of air across samples. Statistical analysis results of elastic elongation are given in Table 4.

4 CONCLUSION

In this research we concluded that:

As the size of circumference of leg at ankle and calf portion increases, the exertion of reverse pressure increases which can be recommended to those patients who needs intensive pressure exertion with passage of time. But the limitation we found is increase in graduation % increased to more than 80%. It is studied that it should be moderate not more than 80%. It reduces the rate of flow of blood from ankle to calf portion as the leg size varies increasing reversal pressure.

Air-permeation of all the three socks samples were evaluated and finalized that the socks sample DGIIRIB exhibit excellent results of air permeation as extended up to maximum of 70%.

Acknowledgement: *This project is funded by Technical University of Liberec, department of Clothing Technology under SGS-2018 project. Project reference number is 21246.*

5 REFERENCES

1. Flaud P., Bassez P., Counord J.: Comparative in vitro study of three inter-face pressure sensors used to evaluate medical compression hosiery, Dermatologic Surgery 12, 2010, pp. 1930-1940
2. Harpa R., Piroi C., Radu C.D.: A new approach for testing medical stockings, Tex Res J 80, 2010, pp. 683-695
3. Smith M.W.L., Dalbey J.C.: Gradient compression hosiery knitted using core spun yarns, Patent application 7895863-B2 USA, 2011
4. Partsch H.: The use of pressure change on standing as a surrogate measure of the stiffness of a compression bandage, Eur. Journal of Vascular Endovascular Surgery 30, 2005, pp. 415-421
5. Liu R., Kwok Y.L., Lao T.T.H., et al.: Objective evaluation of skin pressure distribution of graduated elastic compression stockings, Dermatologic Surgery 31, 2005, pp. 615-624
6. Partsch H., Partsch B., Braun W.: Interface pressure and stiffness of ready-made compression stockings: Comparison of in vivo and in vitro measurements, J of Vascular Surgery 44, 2006, pp. 809-814
7. Bera M., Chattopadhay R., Gupta D.: The effects of fibre blend on comfort characteristics of elastic knitted fabrics used for pressure garments, Journal of the Institution of Engineers 95, 2014, pp. 41-47
8. Macintyre L., Baird M.: Pressure garments for use in the treatment of hyper-trophic scars–an evaluation

of current construction techniques in NHS hospitals, Burns 31, 2005, pp. 11-14

9. Chattopadhyay R., Gupta D., Bera M.: Effect of input tension of inlay yarn on the characteristics of knitted circular stretch fabrics and pressure generation, Journal of Textile Institute 103, 2012, pp. 636-642
10. Tsujisaka T., Azuma Y. and Matsumoto Y.I.: Comfort pressure of the top part of men's socks, Textile Research Journal 74, 2004, pp. 598-602
11. RAL-GZ 387/2, Medical Compression Armsleeves, Quality Assurance, RAL Deutsches Institut für Gütesicherung und Kennzeichnung e.V., Sankt Augustin, DE, 2008
12. Seshadri R, Kathryn H., Peter N., Flowood M.: Use of compression stockings in chronic venous disease: patient compliance and efficacy, Ann. Vasc. Surg. 21, 2007, pp. 790-795
13. Gupta D., Chattopadhyay R., Bera M.: Comfort properties of pressure garments in extended state, Indian Journal of Fiber and Textile Research 36, 2011, pp. 415-421
14. Wang Y., Zhang P., Zhang Y.: Experimental investigation the dynamic pressure attenuation of elastic fabric for compression garment, Textile Research Journal 84, 2014, pp. 572-582
15. Majumdar A., Mukhopadhyay S., Yadav R.: Thermal properties of knitted fabrics made from cotton and regenerated bamboo cellulosic fibers, International Journal of Thermal Sciences 49; 2010, pp. 2042-2048
16. Benltoufa S., Fayala F., Cheikhrouhou M., Ben Nasrallah S.: Porosity Determination of jersey structure, AUTEX Res. J. 7(1), 2007, pp. 63-69
17. Dias T., Delkumburewatte G.B.: Changing porosity of knitted structures by changing tightness, Fibers and Polymers 9, 2008, pp. 76-79
18. Nilgün Ö., ArzuMarmaralı S. and Dönmez K,: Effect of yarn properties on thermal comfort of knitted fabrics. International Journal of Thermal Sciences 46, 2007, pp. 1318–1322
19. Bivainyte A., Mikučioniene D.: Investigation on the air and water vapour permeability of double-layered weft knitted fabrics. Fibres & Textiles in Eastern Europe 19(3), 2011: 18: 69-73
20. Ogulata, R.T., Mavruz, S. Investigation of porosity and air permeability values of plain knitted fabrics. Fibres & Textiles in Eastern Europe 2010; 18(82): 71-75

THE STRUCTURE AND PROPERTIES OF POLYPROPYLENE-MODIFIED HALLOYSITE NANOCLAY FIBRES

Z. Tomčíková[1], A. Ujhelyiová[2], P. Michlík[1], Š. Krivoš[1] and M. Hricová[2]

[1]Research Institute for Man-Made Fibres a.s., Štúrova 2, 05921 Svit, Slovak Republic
[2]Slovak University of Technology in Bratislava, Faculty of Chemical and Food Technology, Institute of Natural and Synthetic Polymers, Radlinského 9, 81237 Bratislava, Slovak Republic
tomcikova@vuchv.sk

Abstract: *Due to the dominance of Asian production of standard man-made fibres in the world, a necessity for the sophistication of European fibres and textiles arises. Bulk or surface modification of materials by nanoadditives is one of the most prospective ways how to ensure special mono- and multi-functionality of fibres in clothing and technical textiles. Natural nanotubes of halloysite nanoclay can be modified (M-HNT) by a chemically, biologically and physically active substances like photoluminescent pigments which emits light after the absorption of photons (electromagnetic radiation). In this work, M-HNT nanotubes modified by organic protective photoluminescent pigment have been used. The article presents results of the study of influence of M-HNT content as well as the influence of uniaxial deformation on the supermolecular structure (birefringence, sound velocity in fibres, crystallinity index and crystallinity) and mechanical properties (fineness, Young´s modulus, tenacity and elongation at break) of modified nanocomposite polypropylene (PP) fibres (PP/M-HNT fibres). Color performance of above mentioned PP/M-HNT fibres was investigated under day light (D65) and after illumination with UV lamp. The obtained experimental results undrawn and drawn of PP/M-HNT fibres were compared with PP fibres modified by organic protective photoluminescent pigment and unmodified PP fibre (standard), both prepared under same technological conditions. Our results confirmed that the nanoadditive halloysite nanoclay can be used as a potential carrier of organic protective photoluminescent pigment for PP nanocomposites, including nanocomposite PP fibres with acceptable impact on structure and mechanical properties of modified nanocomposite fibres.*

Keywords: *modified halloysite nanoclay, photoluminescent pigment, PP nanocomposite fibres, structure, mechanical properties, color performance*

1 INTRODUCTION

The global world production of textile fibres increased in 2016 by 1.7% to 95.3 million tons [1]. This includes an increase of 2.8% in the chemical fibre sector to 70.4 mil tons while natural fibres dropped -1.4% to 24.9 mil tons. The production of PP fibres increased in 2016 by 3.0% to 5.5 million tons [2]. In the future, the increase in textile market is expected to reach 106 mil tons in 2020 and almost 139 mil tons in 2030. This amounts to per capita consumption of 13.9 kg in 2020 and 16.7 kg in 2030 and further increase in the volume of world production of man-made fibres up to 75 mil tons in 2020, at an average annual increase of 4% [3, 4].

The 2016 world survey continues to underscore the dominance of Asia in the fibre business. In 2016 Asia accounted for 88.5% of the worldwide chemical fibre production and holds the dominant position in the world production of standard man-made fibres [1]. This implies the necessity of sophistication of European fibre and textile products in today´s highly competitive environment. It particularly concerns the development of special, modified, mono and multi-functional active fibres and textiles necessarily characterized by high functionality, diversification, flexibility and highly effective and environmentally acceptable production [5, 6]. The most perspective way to ensure sophisticated properties of textiles is modification of their mass or surface by nanotechnologies [5, 6]. The most important nanotechnological procedures in the area of textiles include nano-treatment of their surface and nanoadditive addition of the fibres mass during their extrusion (nanocomposite fibres). By these procedures, mono or multi-functional properties of textiles even at low concentrations of nanoadditives can be achieved, which is very beneficial from an economic aspect as well. The world nanocomposites market is highly prospective and its volume in 2015 was estimated to have reached 7.3 billion US$ [6, 7].

Nanocomposite systems based on natural layered silicates, particularly montmorillonite and halloysite nanoclay (HNT), belong to the most significant studied polymer nanocomposites [8-10]. The advantage of halloysite is the shape of the hollow nanotubes with porous inner surface, which makes them suitable to be used as the carrier

of chemically and biologically active substances for polymer nanocomposite systems [11, 12]. This article presents some results from the study of influence of content natural nanoadditive halloysite nanoclay modified by organic protective photoluminescent pigment as well as the influence of uniaxial deformation on the supermolecular structure and basic mechanical properties of undrawn and drawn modified nanocomposite PP fibres prepared by discontinuous technological process. The obtained experimental results of modified nanocomposite PP fibres were compared with the supermolecular structure and mechanical properties of undrawn and drawn PP fibres modified by organic protective photoluminescent pigment prepared under same technological conditions.

2 EXPERIMENTAL AND METHODS

2.1 Materials

Isotactic granulated polypropylene PP (Slovnaft Company) with MFR=27.6 g/10 min; inorganic nanoadditive halloysite nanoclay 685445 - HNT (Applied Minerals Inc.); inorganic nanoadditive HNT modified by organic protective photoluminescent pigment A (content 20.0 wt.%) - M-HNT in cooperation with A1Synth Ltd. Company; PP/M-HNT masterbatch developed by Research Institute for Man-Made Fibres a.s., Svit (M-HNT content 5.0 wt.%, MFR=28.3 g/10 min); PP masterbatch of organic protective photoluminescent pigment A (Radiant Color NV) developed by Research Institute for Man-Made Fibres, a.s. Svit (pigment content 2.0 wt.%, MFR=20.9 g/10 min) were used during fibre preparation process.

2.2 Fibre preparation

The modified nanocomposite PP/M-HNT fibres were prepared from mechanical mixture of PP granulated polymer and PP/M-HNT masterbatch using the classical discontinuous process of spinning and drawing. The laboratory discontinuous line had an extruder with diameter of D=32.0 mm, with a discontinuous one-step drawing process. There were used constant processing conditions as the spinning temperature of 220°C, spinning die 2x25 holes with diameter 0.3 mm, final spinning process speed of 1500 m.min^{-1}, the drawing ratio λ=2.0, the drawing temperature of 132°C and final drawing process speed of 100 m.min^{-1}. The modified PP/A fibres which were used for comparison, have been prepared from mechanical mixture of PP granulated polymer and PP masterbatch of organic protective photoluminescent pigment A under same processing conditions.

2.3 Methods used

Orientation of fibre (the fibre´s birefringence)

The orientation of macromolecular chains segments in fibre expresses the level of anisotropy of oriented polymer system (fibre). The total orientation of prepared modified nanocomposite PP fibres was evaluated using a DNP 714BI polarization microscope, where the refractive indexes of light in the fibre axis ($n_{//}$) and in the perpendicular direction of the fibre ($n_{\perp}$) were identified. The fibre's birefringence (Δn) was calculated from these values using Equation 1 below:

$$\Delta n = n_{//} - n_{\perp} \quad (1)$$

The sound velocity in fibres

The sound velocity in fibres is given as the ratio of fibre length to the time needed for the transfer of acoustic nodes along that length (expressed in km.s^{-1}). It is dependent on the internal structure arrangement of fibres (expressed by a supermolecular structure parameter) and may serve as a measure of fibre anisotropy. The sound velocity in fibres was measured using a PPMSR Dynamic Modulus Tester (USA).

Crystallinity index (FT-IR)

Crystallinity index I_k of PP fibres represents the fraction of the crystalline phase in PP fibres. It is determined as the ratio of integrated absorbance of absorption band of 840 cm^{-1} (A_{i840}) characterizing the regularity of the arrangement of macromolecular chains segments and integrated absorbance of absorption band of 2723 cm^{-1} (A_{i2723}) as the internal standard influencing the degree of crystallinity:

$$I_k = \frac{A_{i840}}{A_{i2723}} \quad (2)$$

Crystallinity index of modified nanocomposite PP fibres was evaluated by FT-IR spectrophotometer 8400 Shimadzu.

Crystallinity of fibres

Crystallinity β represents the crystalline portion of fibres and may be evaluated by various methods. In this work DSC 4 apparatus Perkin Elmer was used for the evaluation of thermal properties of modified nanocomposite PP fibres and modified PP fibres according to the STN EN ISO 3146/AC. In this procedure the non-isothermal process of analysis was performed. A sample of original fibre was heated by rate of 10°C.min^{-1} from 50 to 260°C. All measurements were carried out in nitrogen atmosphere. Melting enthalpy (ΔH_m) from melting endotherm of 1st heating was determined and was used for the calculation of crystallinity β using the equation 3:

$$\beta = \frac{\Delta H_m}{\Delta H_{m,0}} \cdot 100\% \quad (3)$$

where $\Delta H_{m,0}$ = 198.11 kJ.kg^{-1} is the melting enthalpy of PP with the 100% crystallinity.

Mechanical properties of fibres

The mechanical properties of modified nanocomposite PP fibres and modified PP fibres were measured using Instron 3343 equipment (USA) with a gauge length of 125 mm and clamping rate of 500 $mm.min^{-1}$. The average of at least 10 individual measurements was used for each fibre. The mechanical characteristics (tenacity at break, elongation at break and Young's modulus) were determined according to ISO 2062:1993 and fineness according to the STN EN ISO 1973.

3 RESULTS AND DISCUSSION

From experimental spinning and drawing tests of the studied modified nanocomposite PP system it follows that the PP/M-HNT nanocomposite is fibre forming in over the entire evaluated concentration range of the modified nanofiller (0.05-1.50 wt.%). The discontinuous spinning and drawing processes at drawing ratio λ=2.0 of PP/M-HNT nanocomposite fibres are stable, comparable to unmodified PP standard. The supermolecular structure parameters and basic mechanical properties of pure and nanocomposite undrawn and drawn PP fibres were evaluated.

The obtained results in Tables 1-4 show the effect of the modified nanoadditive (M-HNT) content on the supermolecular structure parameters and mechanical properties of undrawn and drawn nanocomposite PP fibres. It was found, that evaluated concentration range of 0.05-1.5 wt.% of the modified nanofiller M-HNT does not influence significantly the birefringence of undrawn nanocomposite PP fibres (Table 1 - Δn). With an increase of M-HNT content it slightly decreases the crystalline portion β, which is a result of steric braking effect of nanoadditive particles (in nanotubes form) on orientation of segments of PP macromolecular chains into the direction of the fibre axis in the spinning zone. This also implies a slight decrease in the crystalline portion β (Table 1 - β) of PP matrix of undrawn nanocomposite fibres with an increased content of the nanoadditive in the mass of fibres. At the same time, there is slight increase of the sound velocity (Table 1 - average orientation *c*), as well as conformational regularity of their crystalline regions (Table 1 - crystallinity index I_k). It is probably a result of the nucleating effect of nanofiller particles in the process of formation of undrawn nanocomposite PP fibres in the spinning zone.

The uniaxial deformation of undrawn nanocomposite PP fibres significantly increases total average orientation of macromolecular chains of polymer matrix and orientation of macromolecular chains in surface layers (Table 2 - Δn, *c*), as well as crystalline portion β and conformational regularity of crystalline regions (Table 2 - β, I_k) of PP matrix of drawn nanocomposite fibres.

In comparison with drawn unmodified PP fibre, evaluated concentration range 0.05-1.5 wt.% of the modified nanofiller M-HNT in the drawn nanocomposite PP fibres does not influence significantly on the total average orientation of macromolecular chains of polymer matrix and orientation of macromolecular chains in surface layers (Table 2 - Δn, *c*) of drawn nanocomposite PP fibres. At the same time the increased nanoadditive content in the drawn nanocomposite PP fibres results in the decrease in conformational regularity of crystalline regions, as well as crystalline portion β (Table 2 - I_k, β) of drawn nanocomposite fibres. It is probably a result of a steric braking effect of nanoadditive particles (nanotubes form) on orientation of segments of PP macromolecular chains in the direction of the fibre axis in the drawing process of nanocomposite fibres.

Table 1 Supermolecular structure parameters of undrawn PP/M-HNT nanocomposite fibres

Content of M-HNT [wt.%]	$\Delta n.10^3$	$CV_{\Delta n}$ [%]	c [km/s]	CV_c [%]	I_k (FT-IR)	CV_{Ik} [%]	β
-	21.68	1.0	1.88	1.1	1.04	4.0	0.426
0.05	21.66	1.0	1.85	1.2	1.01	3.7	0.425
0.25	21.74	1.2	1.86	1.5	1.05	1.6	0.422
0.50	22.37	0.8	1.90	1.6	1.16	1.8	0.421
0.75	22.34	1.0	1.93	0.7	1.21	4.0	0.416
1.0	22.45	1.1	1.95	1.1	1.22	2.0	0.409
1.5	21.49	1.2	1.94	0.9	1.23	9.6	0.406

Table 2 Supermolecular structure parameters of drawn PP/M-HNT nanocomposite fibres

Content of M-HNT [wt.%]	$\Delta n.10^3$	$CV_{\Delta n}$ [%]	c [km/s]	CV_c [%]	I_k (FT-IR)	CV_{Ik} [%]	β
-	30.26	1.1	2.61	1.8	1.27	3.7	0.448
0.05	29.68	0.9	2.56	1.3	1.27	4.9	0.445
0.25	30.34	1.1	2.58	1.9	1.23	1.2	0.440
0.50	30.59	1.1	2.59	1.8	1.25	1.1	0.435
0.75	30.64	1.6	2.61	1.8	1.17	3.8	0.432
1.0	30.66	1.7	2.62	1.5	1.12	1.4	0.427
1.5	30.51	1.9	2.60	1.9	1.09	0.7	0.423

Table 3 Mechanical properties of undrawn PP/M-HNT nanocomposite fibres

Content of M-HNT [wt.%]	Fineness [dtex]	CV_F [%]	Tenacity [cN/dtex]	CV_T [%]	Elongation [%]	CV_E [%]	Young´s modulus [cN/dtex]	CV_{YM} [%]
-	460.8	0.6	2.1	4.2	268.7	5.6	11.4	8.5
0.05	460.2	0.9	2.1	4.6	285.8	5.5	12.2	8.6
0.25	459.5	1.1	2.1	3.8	288.3	6.3	12.9	8.6
0.50	460.3	0.9	2.0	3.4	271.2	5.1	14.7	8.7
0.75	462.3	1.3	2.0	4.6	279.2	5.1	17.0	4.2
1.0	461.5	0.9	1.9	4.4	279.0	6.7	17.6	5.3
1.5	462.5	1.3	1.9	3.1	282.8	5.0	18.8	7.8

Table 4 Mechanical properties of drawn PP/M-HNT nanocomposite fibres

Content of M-HNT [wt.%]	Fineness [dtex]	CV_F [%]	Tenacity [cN/dtex]	CV_T [%]	Elongation [%]	CV_E [%]	Young´s modulus [cN/dtex]	CV_{YM} [%]
-	255.7	2.4	4,1	2.3	103.4	3.9	40.1	3.2
0.05	258.3	1.2	4,0	1.6	100.4	3.7	39.8	3.5
0.25	258.6	0.9	3,9	2.1	95.4	6.2	40.6	3.5
0.50	257.7	1.2	3,9	2.4	94.2	6.5	38.7	2.3
0.75	259.6	1.2	3,7	2.9	90.1	5.6	38.9	4.5
1.0	260.4	0.8	3,6	2.1	92.5	7.4	38.4	3.8
1.5	259.8	1.4	3,5	1.2	92.2	4.8	36.2	3.7

The fineness of undrawn PP/M-HNT nanocomposite fibres was found constant and does not depend on M-HNT content in the fibres (Table 3). The slight increase in their elongation (up to 20% absolute) and slight decrease in their tenacity (up to 10%) when compared to unadditivated standard was found. An increase in Young's modulus with increased M-HNT content in the mass of undrawn fibres (up to 20%) is mainly related to the increase in the conformational regularity of their crystalline areas (Table 1 - I_k).

The fineness of drawn PP/M-HNT nanocomposite fibres was found constant in dependence of M-HNT content in the fibres (Table 4). The process of uniaxial deformation of undrawn nanocomposite fibres significantly increases the tenacity and Young´s modulus and decreases elongation of drawn fibres. It is the result of a significant increase in total average orientation of macromolecular chains of polymer matrix and orientation of macromolecular chains in surface layers (Table 2 - Δn, c), crystalline portion β also the crystallinity index of PP matrix (Table 2 - β, I_k) of drawn nanocomposite fibres.

With increased nanoadditive content in the mass of drawn PP/M-HNT nanocomposite fibres slight decreases the tenacity (up to 15 %), the elongation (up to 15 % absolute) and the Young's modulus (up to 10 %) of drawn fibres (Table 4). It is mainly related to the decrease in conformational regularity of crystalline areas and crystaline portion β (Table 2 - I_k, β) of drawn nanocomposite fibres.

Obtained values of the basic mechanical properties of PP/M-HNT nanocomposite fibres are in good correlation with evaluated parameters of their supermolecular structure.

Figures 1 and 2 show the effect of the modified nanofiller M-HNT content on the color performance of undrawn and drawn nanocomposite PP/M-HNT fibres under daylight D65 (a) and under a UV lamp.

a) b)

Figure 1 The influence of modified nanofiller M-HNT with a content 0.05; 0.25; 0.50 and 1.50 wt.% on the color performance of undrawn nanocomposite PP fibres compared with unmodified PP fibre (first from the left) under daylight D65 (a) and under a UV lamp (b)

a) b)

Figure 2 The influence of modified nanofiller M-HNT with a content 0.05; 0.25; 0.50; 1.00 and 1.50 wt.% on the color performance of drawn nanocomposite PP fibres compared with unmodified PP fibre (first from the left) under daylight D65 (a) and under a UV lamp (b)

Figures 1a and 2a clearly show that all prepared PP/M-HNT nanocomposite fibers are white under the daylight D65. Under the UV lamp there is no shine to only in the case of unmodified PP fibre (Figures 1b and 2b) while the nanocomposite PP fibres with M-HNT turn blue. Color intensity increases as the content of modified nanofiller M-HNT in nanocomposite PP fibres is increased. It is evident from Figures 1b and 2b that even at low content of M-HNT (about 0.05 wt.%, samples 2 from left to right) a clearly visible color change under the UV lamp is provided.

From the experimental spinning and drawing tests of the modified PP/A fibres which were used for comparison it follows that the modified system is fibre forming in over the entire evaluated concentration range 0.01-0.30 wt.% of photoluminescent pigment A in the mass of PP/A fibre. The discontinuous spinning and drawing processes at drawing ratio λ=2.0 of PP/A modified fibres are stable, comparable to unmodified PP standard. The supermolecular structure parameters and basic mechanical properties of pure and modified undrawn and drawn PP fibres were evaluated.

The obtained results in Tables 5-8 show the effect of the photoluminescent pigment A content on the supermolecular structure parameters and mechanical properties of undrawn and drawn PP/A modified fibres.

In the case of undrawn PP/A modified fibres a slight increasing in dependence of birefringence and sound velocity (Table 5 - Δn, c) and slight decreasing in dependence of crystalline portion β and conformational regularity of crystalline regions (Table 5 - β, I_k) on the photoluminescent pigment A content was found.

The uniaxial deformation of undrawn PP/A modified fibres significantly increases total average orientation of macromolecular chains in polymer matrix and orientation of macromolecular chains in surface layers (Table 6 - Δn, c), as well as crystalline portion β and conformational regularity of crystalline regions (Table 6 - β, I_k) in PP matrix of drawn modified fibres.

In comparison with drawn unmodified PP fibre, the evaluated concentration range 0.01-0.30 wt.% of the photoluminescent pigment A in the drawn PP/A modified fibres slightly increases total average orientation of macromolecular chains in polymer matrix (Table 6 - Δn). At the same time, the increased pigment A content in the drawn modified PP fibres results in the slight increase in conformational regularity of crystalline regions and decrease the crystalline portion β (Table 6 - I_k, β) of drawn modified fibres. It is probably the result of a plasticizing effect of organic photoluminescent pigment A on orientation of PP macromolecular chain segments in the direction of the fibre axis in the drawing process of modified fibres.

Table 5 Supermolecular structure parameters of undrawn PP/A modified fibres

Content of pigment A [wt.%]	$\Delta n.10^3$	$CV_{\Delta n}$ [%]	c [km/s]	CV_c [%]	I_k (FT-IR)	CV_{Ik} [%]	β
-	20.48	2.1	1.79	0.6	1.10	0.4	0.425
0.01	20.71	1.2	1.86	0.5	1.20	0.2	0.422
0.05	21.00	1.1	1.87	1.0	1.13	0.1	0.420
0.10	21.37	0.9	1.87	0.3	1.16	0.1	0.419
0.15	21.69	1.5	1.88	0.7	1.04	0.1	0.417
0.20	22.12	0.8	1.89	0.9	1.01	0.1	0.413
0.30	21.86	1.4	1.88	1.4	1.04	0.1	0.410

Table 6 Supermolecular structure parameters of drawn PP/A modified fibres

Content of pigment A [wt. %]	$\Delta n.10^3$	$CV_{\Delta n}$ [%]	c [km/s]	CV_c [%]	I_k (FT-IR)	CV_{Ik} [%]	β
-	29.37	0.8	2.54	1.4	1.45	0.4	0.451
0.01	32.07	1.2	2.59	1.4	1.46	0.7	0.448
0.05	33.57	1.3	2.61	1.5	1.54	0.3	0.443
0.10	33.75	1.4	2.64	1.2	1.64	0.3	0.442
0.15	34.21	1.5	2.67	1.4	1.72	0.1	0.441
0.20	33.81	0.7	2.60	1.3	1.63	0.1	0.435
0.30	33.15	0.8	2.53	1.1	1.54	0.1	0.430

Table 7 Mechanical properties of undrawn PP/A modified fibres

Content of pigment A [wt. %]	Fineness [dtex]	CV_F [%]	Tenacity [cN/dtex]	CV_T [%]	Elongation [%]	CV_E [%]	Young´s modulus [cN/dtex]	CV_{YM} [%]
-	450.6	1.0	2.1	3.1	284.1	6.6	10.6	16.7
0.01	444.2	1.0	2.1	5.2	276.7	8.3	11.1	16.5
0.05	448.5	1.3	2.1	2.7	297.8	4.9	11.4	15.3
0.10	445.1	0.5	2.1	3.1	291.0	6.7	12.6	5.9
0.15	443.5	0.5	2.1	2.6	307.6	4.8	13.5	7.8
0.20	444.4	0.7	2.0	5.0	309.8	7.3	15.3	6.7
0.30	442.5	0.8	1.9	4.1	311.5	9.4	17.4	6.6

Table 8 Mechanical properties of drawn PP/A modified fibres

Content of pigment A [wt. %]	Fineness [dtex]	CV_F [%]	Tenacity [cN/dtex]	CV_T [%]	Elongation [%]	CV_E [%]	Young´s modulus [cN/dtex]	CV_{YM} [%]
-	247.8	1.5	4.0	2.3	84.6	6.2	38.6	3.0
0.01	245.5	2.4	4.1	3.0	89.0	7.0	37.9	2.2
0.05	245.4	1.6	4.1	4.4	89.9	10.5	38.3	4.3
0.10	245.8	0.5	3.9	3.4	93.0	7.1	37.0	1.7
0.15	243.3	0.8	3.8	3.8	96.0	11.3	36.6	4.0
0.20	244.7	1.8	3.8	3.8	101.8	11.2	35.3	3.3
0.30	242.3	0.7	3.7	2.9	108.2	9.9	35.0	5.3

The fineness of undrawn PP/A modified fibres was found constant in dependence of pigment A content in the fibres (Table 7). The slight increase in their elongation (up to 25% absolute) and slight decrease in their tenacity (up to 10%) when compared to unmodified standard was found. An increase in Young's modulus with increased pigment A content in the mass of undrawn fibres is probably related to the slight increase of their birefringence and sound velocity (Table 5 - Δn, c).

The fineness of drawn PP/A modified fibres was found constant in dependence of pigment A content in the fibres (Table 8), as well. The process of uniaxial deformation of undrawn PP/A modified fibres significantly increases the tenacity and the Young´s modulus of drawn fibres. It is the result of a significant increase in total average orientation of macromolecular chains of polymer matrix and orientation of macromolecular chains in surface layers (Table 5 - Δn, c), crystalline portion β also the crystallinity index of PP matrix (Table 5 - β, I_k) of drawn nanocomposite fibres.

With increased pigment A content in the mass of drawn PP/A modified fibres slightly decreases the tenacity (up to 8%), the Young's modulus (up to 10%) and slightly increases the elongation (up to 20% absolute) of drawn modified fibres (Table 8).

Figures 3a and 4a show that all prepared PP/A modified fibers under the daylight D65 are white. Under the UV lamp there is only unmodified PP (Figures 3b and 4b) not shiny, while the modified PP fibres with photoluminescent pigment A turn to blue. Color intensity increases as the content of photoluminescent pigment A in modified PP fibres is increased. It is evident from Figures 3b and 4b that even the lowest pigment A content (about 0.01 wt.%, samples 2 from left to right) provides a clearly visible color change under the UV lamp.

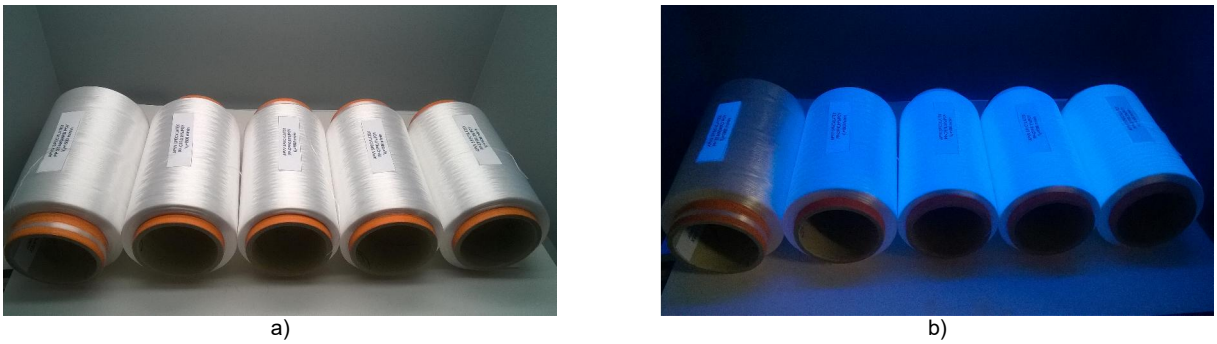

a) b)

Figure 3 The influence of photoluminescent pigment A with content 0.01; 0.05; 0.10 and 0.30 wt.% on the color performance of undrawn PP/A modified fibres compared with unmodified PP fibre (first from the left) under daylight D65 (a) and under a UV lamp (b)

a) b)

Figure 4 The influence of photoluminescent pigment A with content 0.01; 0.05; 0.10; 0.20 and 0.30 wt. % on the color performance of drawn PP/A modified fibres compared with unmodified PP fibre (first from the left) under daylight D65 (a) and under a UV lamp (b)

4 CONCLUSION

The results from the study of the spinning, drawing, supermolecular structure and mechanical properties of modified PP/M-HNT nanocomposite fibres presented in this article have showed that the modified nanocomposite system PP/modified halloysite is fibre forming using discontinuous technological process in the whole evaluated range 0.05-1.50 wt.% of modified halloysite nanoparticles. The technological conditions for stable spinning and drawing were found. The basic dependences of the influence of modified nanoadditive content and uniaxial deformation on the supermolecular structure parameters and basic mechanical properties of undrawn and drawn modified nanocomposite PP fibres were evaluated. Addition of modified halloysite into PP fibres does not influence significantly the total average orientation of macromolecular chains of polymer matrix, at the same time reduces the crystallinity, as well as the conformational regularity of crystalline regions of oriented nanocomposite fibres. This led to the slight decrease in the tenacity (up to 15%), the elongation (up to 15% absolute) and the Young's modulus (up to 10%) of drawn nanocomposite fibres. Influence of content 0.05-1.50 wt.% of modified halloysite by the photoluminescent pigment A (M-HNT) on the supermolecular structure and mechanical properties drawn PP fibres is practically comparable with the influence of content 0.01-0.30 wt.% of photoluminescent pigment A in drawn PP fibres.

An important result is also the finding that the color performance under the UV light is clearly visible even at lowest modified halloysite content (0.05 wt.%) in modified PP/M-HNT nanocomposite fibres. Color intensity increases as the content of modified halloysite M-HNT in nanocomposite PP fibres is increased. Their color performance under the UV lamp there is comparable with the color performance of PP fibres modified by the photoluminescent pigment A with content of 0.01-0.30 wt.%. Therefore, it can be used as a tool for protection of original PP fibres and textile products.

Based on the obtained results it can be stated that the evaluated nanoadditive halloysite nanoclay proves to be a potential carrier of chemically and biologically active modifying substances for PP nanocomposites, including nanocomposite PP fibres with acceptable impact on structure and mechanical properties of modified nanocomposite fibres.

ACKNOWLEDGEMENT: *This work was supported by the Slovak Research and Development Agency under the contract No. APVV-14-0175.*

5 REFERENCES

1. An.: Global fiber production, Man-Made Fiber Year Book 2017, 67, 2017, pp. 27-29
2. An.: Global fiber production, Chemical Fibers International, 67(4), 2017, pp. 195-197
3. Engelhardt, A.: Analysis of per capita fiber consumption, International Fiber Journal, 27(5), 2013, pp. 4-8
4. An.: Man-made fiber production 2020, Chemical Fibers International, 63(1), 2013, p. 20
5. Purvis, C.: Challenges in the global man-made fibers market, Proceedings of 49th Dornbirn Man-Made Fibers Congress - Congress-Guide, Dornbirn, September 2010, p. 48
6. De Schrijver, I. et al: Nanotechnology in demanding textile applications, Proceedings of 48th Dornbirn Man-Made Fibers Congress - Congress-Guide, Dornbirn, September 2009, p. 63
7. Sezen, M.: Nanotechnology and nanotextiles: technologies, markets, economics and future trends, Proceedings of 48th Dornbirn Man-Made Fibers Congress - Congress-Guide, Dornbirn, September 2009, p. 66
8. Joussein, E. et al: Halloysite clay minerals – A review, Clay Minerals, 40(4), 2005, pp. 383-426, ISSN 0009-8558
9. Du, M. et al: Newly emerging applications of halloysite nanotubes: A review, Polymer Int., 59(5), 2010, pp. 574-582
10. Lvov, Y; Abdullayev, E: Functional polymer-clay nanotube composites with sustained release of chemical agents, Progress in Polymer Science, 38(10-11), 2013, pp. 1690-1719
11. Khunová, V. et al: The effect of halloysite modification combined with in situ matrix modifications on the structure and properties of polypropylene/halloysite nanocomposites, eXPRESS Polymer Letters, 7(5), 2013, pp. 471-479
12. Liu, M et al: Recent advance in research on halloysite nanotubes-polymer nanocomposite, Progress in Polymer Science, 39(8), 2014, pp. 1498-1525

INSTRUCTIONS FOR AUTHORS

The journal ,,**Vlákna a textil**" (**Fibres and Textiles**) is the scientific and professional journal with a view to technology of fibres and textiles, with emphasis to chemical and natural fibres, processes of fibre spinning, finishing and dyeing, to fibrous and textile engineering and oriented polymer films. The original contributions and works of background researches, new physical-analytical methods and papers concerning the development of fibres, textiles and the marketing of these materials as well as review papers are published in the journal.

Manuscript

The original research papers are required to be written in English language with summary. The advertisements will be published in a language according to the mutual agreement.

The first page of the manuscript has to contain:

The title of the article (16 pt bold, capital letters, centred)

The full *first name* (s) and also *surnames* of all authors (11 pt, bold, centred).

The complete address of the working place of the authors, e-mail of authors (9 pt, italic, centred)

Abstract (9 pt, italic)

Key words (9 pt, italic)

The manuscript has to be written in A4 standard form, in **Arial, 10 pt**.

The text should be in ***double-column format*** *(width 8.1 cm)* ***in single line spacing.***

Page margins: up and down 2.5 cm; left and right 2.0 cm.

Do not number the pages and do not use footnotes. Do not use business letterhead.

Figures, tables, schemes and photos (centered) should be numbered by Arabic numerals and titled over the table and under the figure or picture.

Photos and schemes have to be sufficiently contrastive and insert in text as pictures.

Figures, tables, schemes and photos, please, send in separate file.

Mathematical formulae should be centred on line and numbered consecutively on the right margin.

Physical and technical properties have to be quantified in SI units, names and abbreviations of the chemical materials have to be stated according to the IUPAC standards.

References in the text have to be in square brackets and literature cited at the end of the text. References (9 pt), have to contain names of all authors.

[1] Surname N., Surname N.: Name of paper or Chapter, In Name of Book, Publisher, Place of Publication, YYYY, pp. xxx-yyy

[2] Surname N., Surname N.: Name of paper, Name of Journal Vol. (No.), YYYY, pp. xxx-yyy

[3] Surname N., Surname, N.: Title of conference paper, Proceedings of xxx xxx, conference location, Month and Year, Publisher, City, Surname N. (Ed.), YYYY, pp. xxx-yyy

[4] Surname N., Surname N.: Name of Paper, Available from http://www.exact-address-of-site, Accessed: YYYY-MM-DD

The final template of manuscript is available on **http://www.vat.ft.tul.cz**

Authors are kindly requested to deliver the paper (in Word form) to be published together with information about at least 3 recommended reviewers from institutions others than the parent (name, e-mail, institution, department) by e-mail: marcela.hricova@stuba.sk

After successful review procedure there is charged fee (article processing charge) of EUR 100. All articles after review process are freely available online and this fee helps to cover the costs of taking a manuscript and turning it into a finished article.

Address of the Editor Office:

Marcela Hricová

Faculty of Chemical and Food Technology,

Slovak University of Technology in Bratislava

Radlinskeho 9

812 37 Bratislava,

Slovakia